A Four-Component Domino Reaction: An Eco-Compatible and Highly Efficient Construction of 1,8-Naphthyridine Derivatives, their *In-Silico* molecular docking, Drug likeness, ADME and Toxicity studies

Ankita Garg[a], Aschalew Tadesse[a], Rajalakshmanan Eswaramoorthy[a]*

[a]Department of Applied Chemistry, School of Applied Natural Science, Adama Science and Technology University, Adama, P.O. 1888, Ethiopia.

rajalakshmanan.e@gmail.com; ankitagargchem@gmail.com

Table of Contents

1. Experimental Section

1.1. General

^{1}H NMR and ^{13}C NMR spectra were recorded on Jeol Resonance ECX-400II (400 MHz); Chemical shifts (δ in ppm) and coupling constant (*J* in Hz) are calibrated either relative to internal solvent tetramethylsilane TMS (δ_H = 0.00 ppm) or DMSO-d_6 (δ_H = 3.33 ppm). In the ^{1}H NMR data, the following abbreviations were used throughout: *s* = singlet, *d* = doublet, *t* = triplet, *dd* = double doublets, *m* = multiplet and *brs* = broad singlet. In the ^{13}C NMR spectra, chemical shifts are calibrated relative to DMSO-d_6 (δ_C = 39.51 ppm). The High-Resolution Mass Spectra (HRMS) was performed on Bruker daltronics microTOF-QII® spectrometer using ESI ionization. IR spectra were recorded on Perkin Elmer FT-IR spectrometer- spectrum two. Melting points were performed with *Optimelt* automated melting point system.

The reactions were performed in a G-10 Borosilicate glass vial sealed with Teflon septum in Anton Paar Monowave 300 reactor®, operating at a frequency of 2.455 GHz with continuous irradiation power of 0 to 300 W. Analysis of the reactions were done by thin layer chromatography (TLC) on Merck precoated silica gel TLC plates (Merck® 60F_{254}). Chemicals and reagents were purchased from Sigma Aldrich and Alfa Aesar. All solvents, ethanol, petroleum ether, ethyl acetate were purchased from locally available commercial sources and used as received.

*1.2. General procedure for the synthesis of products (**6a-i**)*

A mixture of enaminone **3** (1.0 mmol), malononitrile **4** (2.2 mmol, 2.2 equiv) and *o*-phthalaldehyde **5** (1.0 mmol) was introduced in a G-10 glass vial capped with a Teflon septum and was subjected to microwave irradiation with the initial ramp time of 1 min. at 60 °C and then the temperature was raised to 110 °C with a holding time of 20 min. with DMF (2 mL) as a solvent. The reaction was monitored by TLC. After the completion, the reaction mixture was then cooled to room temperature and diluted with cold water (40 mL), then filtered, the precipitate was collected and purified by recrystallization from 95% EtOH except 6h which was purified by silica gel column chromatography (eluent 15-20% ethyl acetate/pet. ether). The analytical data for represent compounds are shown below from S7-S10.

1.3. In silico molecular docking Methodology

1.3.1. Preparation of ligands

The 2D structures (.mol) of all synthesized compounds (**6a-i**) were drawn and each individual structure was analyzed by using ChemDraw 16.0. All the compounds (**6a-i**) were converted to 3D structure (.pdb) using Chem3D 16.0. The 3D coordinates (.pdb) of each molecule were loaded on to Chem3D for energy minimization.

1.3.2. Preparation of macromolecule

The crystal structure of receptor molecule *E. coli* gyraseB (PDB ID: 6F86) and human topoisomerase IIβ with DNA (PDB ID 3QX3) were downloaded from protein data bank. The protein preparation was done using the reported standard protocol [1] by removing the co-crystallized ligand, selected water molecules and cofactors, the target protein file was prepared by leaving the associated residue with protein by using Auto Preparation of target protein file Auto Dock 4.2 (MGL tools1.5.7).

1.3.3. Autodock Vina analysis

The graphical user interface program Auto Dock 4.2 was used to set the grid box for docking simulations. The grid was set so that it surrounds the region of interest in the macromolecule. The docking algorithm provided with Auto Dock Vina was used to search for the best docked conformation between ligand and protein. During the docking process, a maximum of nine conformers were considered for each ligand. The conformations with the most favorable (least) free binding energy were selected for analyzing the interactions between the target receptor and ligands by Discovery studio visualizer and PyMOL. The ligands are represented in different color, H-bonds and the interacting residues are represented in stick model representation.

Reference

[1] Narramore, S., Stevenson, C. E. M., Maxwell, A., Lawson, D. M., Fishwick, C. W. G., 2019. New insights into the binding mode of pyridine-3-carboxamide inhibitors of E. coli DNA gyrase. Bioorg. Med. Chem. 27, 3546–3550. https://doi.org/10.1016/j.bmc.2019.06.015

2. Green Metrics

2.1. Scheme and General Calculation

(A) Calculation for the synthesis of 6-amino-4-(4-methoxyphenyl)-1-oxo-1,2,3,4,7a,11b-hexahydro-4a1H-cyclopenta[b]indeno[1,2,3-de][1,8]naphthyridine-4a1,7-dicarbonitrile **6c**

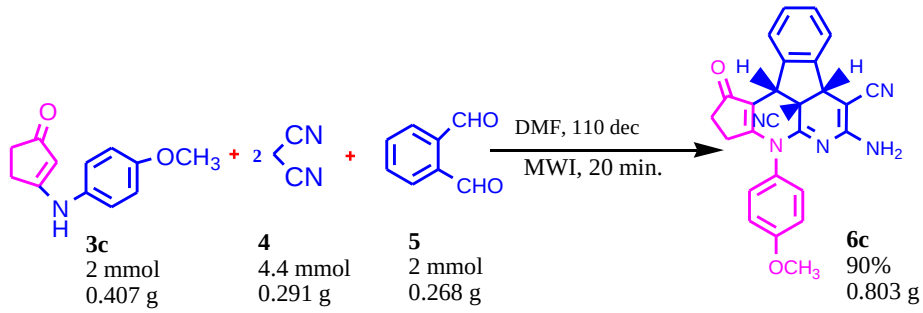

3c
2 mmol
0.407 g

4
4.4 mmol
0.291 g

5
2 mmol
0.268 g

6c
90%
0.803 g

Raw Materials Used		**Crude Product and Waste**	
3-(4-methoxyphenylamino)cyclopent-2-enone (1.0 eq.)	0.407 g	Product	0.803 g
Malononitrile (2.0 eq.)	0.291 g	Waste	3.163 g
Phthaldialdehyde (1.0 eq.)	0.268 g		
DMF	3 ml		
Total	3.966 g	**Total**	3.966 g

2.2. Individual Calculation for various factors

(i) Atom Economy (AE): Atom Economy measures the efficiency of a chemical reaction with regard to how many atoms from the starting materials reside within the desired product. The ideal value for AE should be 100%

$$AE = \frac{(Mol\ Wt.\ of\ all\ reactants)}{(Mol\ Wt.\ of\ Product)}\ x\ 100$$

$$= \frac{433.4614}{203.24 + 66.06 + 66.06 + 134.14}$$

$$= 92.32\ \%$$

(ii) Carbon Efficiency (CE): Carbon Efficiency is defined as mass ratio of carbon in the desired product to the total carbon present in the reactants.

$$CE = \frac{[(mmol.\ of\ Product)\ x\ No.\ of\ Carbons]}{(mmol.\ of\ all\ reactants\ x\ No.\ of\ Carbons)}\ x\ 100$$

$$= \frac{1.86 \text{ x } 26}{(2 \text{ x } 12) + (4.4 \text{ x } 6) + (2 \text{ x } 8)}$$

$$= 72.83$$

(iii) Reaction Mass Efficiency (RME): Reaction Mass Efficiency is defined as the mass of desired product divided by total mass of reactants in the stoichiometric equation. The ideal value for RME should be 100%.

$$RME = \frac{(Wt.\ of\ Product)}{(Total\ Wt.\ of\ all\ reactants)}\ x\ 100$$

$$= \frac{0.803}{(0.407 + 0.291 + 0.268)}\ \text{x}\ \ 100$$

$$= 83.13$$

(iv) E-Factor: E-Factor is defined as the mass ratio of waste to desired product. The ideal value for E factor should be zero.

$$E\text{ - }Factor = \frac{(Total\ Waste)}{(desired\ Product)}$$

$$= \frac{3.163\ \text{g}}{0.803\ \text{g}}$$

$$= 3.938$$

(v) Process Mass Intensity (PMI): Process Mass Intensity is defined as the total mass used in a process divided by the mass of desired product. The ideal value for PMI should be 1.

$$PMI = \frac{Raw\ Materials}{Crude\ Product}$$

$$= \frac{3.966\ g}{0.803\ g}$$

$$= 4.938$$

3. The theory calculation of intermediate B

We have calculated possible configurations of the intermediate *syn*-**B** and *anti*-**B** by energy minimization calculation using Monte Carlo Force Field (MMFF94). The lowest energy corresponds to the configurations were calculated. The results are shown in Figure 1. From Figure 1, we found that the most stable configuration of *syn*-**B** is 20 cal/mol lower in energy than configuration of *anti*-**B**.

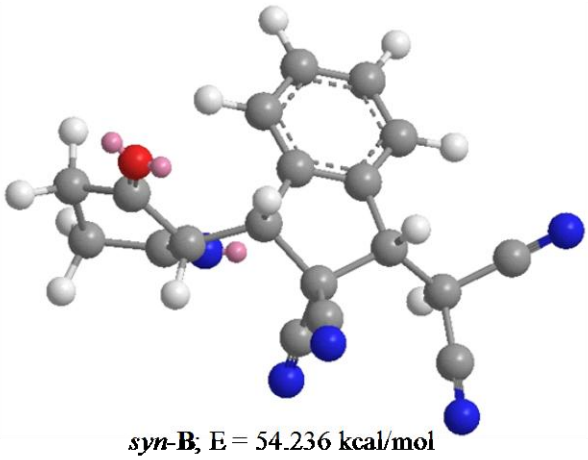

***syn*-B**; E = 54.236 kcal/mol

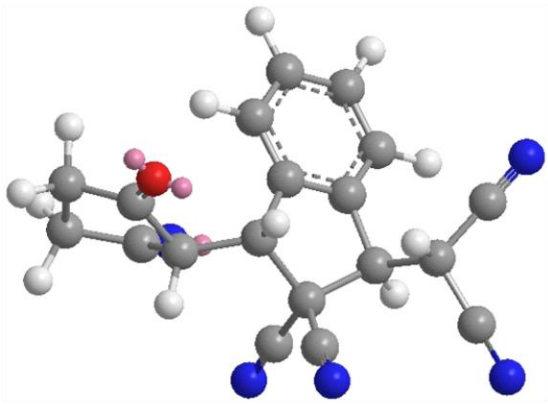

***anti*-B**; E = 54.256 kcal/mol

The lowest energy minimum of the intermediate *syn*-B and *anti*-B

4. Characterization for all compounds

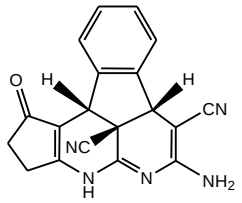

6a

4.1. 6-amino-1-oxo-1,2,3,4,7a,11b-hexahydro-4a1H-cyclopenta[b]indeno[1,2,3-de][1,8]naphthyridine-4a1,7-dicarbonitrile (6a). Yellow solid (89%), 274-276°C; IR (KBr) (4000-600 cm^{-1}): ν_{max}: 3349, 3334, 2960, 2172, 1657, 1628, 1558, 1490, 1378, 1202, 1045, 732, 696. ^{1}H NMR: (400 MHz, DMSO-d_6) δ 2.44 (s, 4H), 4.68 (s, 1H), 4.81 (s, 1H), 6.67 (s, 2H), 7.24-7.42 (m, 4H), 9.22 (brs, NH) ppm. ^{13}C NMR: (100 MHz, DMSO-d_6) δ 26.8, 34.2, 42.7, 46.2, 49.1, 52.8, 115.2, 117.4, 129.2, 129.4, 129.7, 130.0, 130.4, 140.9, 141.3, 154.1, 157.1, 167.8, 202.1 ppm. HR-MS (ESI) for $C_{19}H_{13}N_5O$ m/z calcd.: 328.1154; found: 328.1152 $[M+H]^+$.

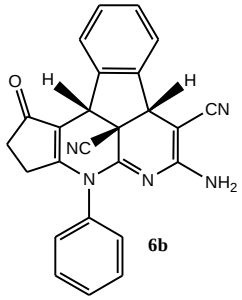

6b

4.2. 6-amino-1-oxo-4-phenyl-1,2,3,4,7a,11b-hexahydro-4a1H-cyclopenta[b]indeno[1,2,3-de][1,8]naphthyridine-4a1,7-dicarbonitrile (6b). Yellow solid (92%), 278-280°C; IR (KBr) (4000-600 cm^{-1}): ν_{max}: 3339, 2957, 2174, 1621, 1591, 1470, 1348, 1278, 1188, 1045, 764, 688. ^{1}H NMR: (400 MHz, DMSO-d_6) δ 2.46 (s, 4H), 4.68 (s, 1H), 4.81 (s, 1H), 6.67 (s, 2H), 7.015 (dd, 2H, J = 20 & 8 Hz), 7.22-7.43 (m, 6H), 7.51 (t, 1H, J = 8Hz) ppm. ^{13}C NMR: (100 MHz, DMSO-d_6) δ 26.5, 34.3, 42.8, 46.3, 49.1, 52.6, 115.2, 117.4, 122.0, 123.4, 123.6, 127.9, 129.2, 129.4, 129.7, 130.0, 130.4, 134.3, 137.3, 141.1, 141.4, 154.1, 157.2, 167.9, 202.3 ppm. HR-MS (ESI) for $C_{25}H_{17}N_5O$ m/z calcd.: 404.1467; found: 404.1471 $[M+H]^+$.

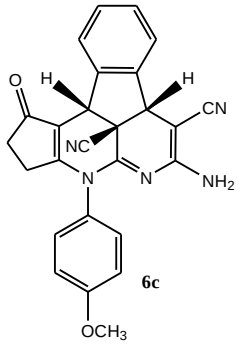

6c

4.3. 6-amino-4-(4-methoxyphenyl)-1-oxo-1,2,3,4,7a,11b-hexahydro-4a1H-cyclopenta[b]indeno[1,2,3-de][1,8]naphthyridine-4a1,7-dicarbonitrile (6c). Yellow solid (93%), >

300°C; IR (KBr) (4000-600 cm^{-1}): ν_{max}: 3336, 2954, 1662, 1589, 1382, 1336, 1248, 1125, 1009, 879, 742, 605. ^{1}H NMR: (400 MHz, DMSO-d_6) δ 3.72 (s, 4H), 4.115 (q, 3H, J = 8 Hz), 4.66 (s, 1H), 4.78 (s, 1H), 6.66 (s, 2H), 6.90 (s, 2H), 7.03 (d, 2H, J = 8 Hz), 7.13 (d, 1H, J = 8 Hz), 7.23- 7.36 (m, 3H) ppm. ^{13}C NMR: (100 MHz, DMSO-d_6) δ 27.1, 29.8, 34.7, 43.2, 46.9, 49.6, 53.4, 115.2, 117.7, 123.0, 123.4, 123.6, 125.0, 127.9, 128.5, 130.0, 130.1, 130.4, 137.6, 140.3, 140.9, 141.3, 154.7, 157.4, 168.5, 202.3 ppm. HR-MS (ESI) for $C_{26}H_{19}N_5O_2$ m/z calcd.: 434.1572; found: 434.1568 $[M+H]^+$.

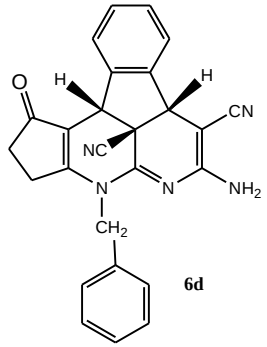

6d

4.4. 6-amino-4-benzyl-1-oxo-1,2,3,4,7a,11b-hexahydro-4a1H-cyclopenta[b]indeno[1,2,3-de][1,8]naphthyridine-4a1,7-dicarbonitrile (6d). Yellow solid (82%), 275-278°C; IR (KBr) (4000-600 cm^{-1}): ν_{max}: 3331, 2958, 2174, 1654, 1631, 1564, 1451, 1338, 1258, 1212, 1168, 735. ^{1}H NMR: (400 MHz, DMSO-d_6) δ 2.47 (s, 4H), 4.06 (s, 2H), 4.68 (s, 1H), 4.85 (s, 1H), 6.67 (s, 2H), 7.04 (d, 2H, J= 8Hz) 7.22-7.42 (m, 6H), 7.51-7.56 (m, 1H,) ppm. ^{13}C NMR: (100 MHz, DMSO-d_6) δ 26.5, 31.6, 42.5, 44.6, 46.1, 48.9, 52.6, 115.2, 115.6, 117.4, 121.8, 123.8, 127.9, 129.0, 129.4, 130.0, 130.4, 130.8, 137.3, 140.3, 140.9, 141.3, 154.1, 157.1, 167.8, 202.1 ppm. HR-MS (ESI) for $C_{26}H_{19}N_5O$ m/z calcd.: 418.1623; found: 418.1634 $[M+H]^+$.

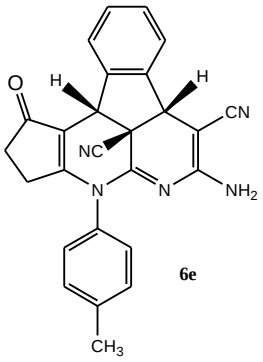

6e

4.5. 6-amino-1-oxo-4-(p-tolyl)-1,2,3,4,7a,11b-hexahydro-4a1H-cyclopenta[b]indeno[1,2,3-de][1,8]naphthyridine-4a1,7-dicarbonitrile (6e). Yellow solid (88%), > 300°C; IR (KBr) (4000-600 cm^{-1}): ν_{max}: 3419, 2954, 2161, 1632, 1605, 1565, 1470, 1380, 1283, 1222, 935, 849, 736, 688. ^{1}H NMR: (400 MHz, DMSO-d_6) δ 3.1325 (dd, 3H, 32 & 16 Hz), 3.72 (s, 4H), 4.66 (s, 1H), 4.78 (s, 1H), 6.66 (s, 2H), 6.97 (s, 2H), 7.02-7.39 (m, 6H) ppm. ^{13}C NMR: (100 MHz, DMSO-d_6) δ 20.1, 26.8, 34.2, 42.7, 46.2, 49.1, 52.8, 115.2, 117.4, 121.8, 123.4, 123.6, 127.9, 129.2, 129.4, 129.7, 130.0, 130.4, 137.4, 139.4, 141.1, 141.4, 155.5, 158.8, 170.1, 200.0 ppm. HR-MS (ESI) for $C_{26}H_{19}N_5O$ m/z calcd.: 418.1623; found: 418.1618 $[M+H]^+$.

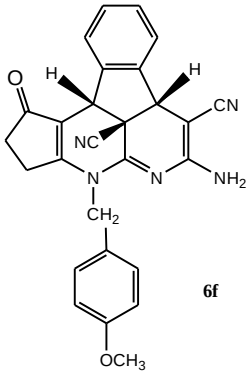

6f

4.6. *6-amino-4-(4-methoxybenzyl)-1-oxo-1,2,3,4,7a,11b-hexahydro-4a1H-cyclopenta[b]indeno[1,2,3-de][1,8]naphthyridine-4a1,7-dicarbonitrile (6f).* Yellow solid (81%), 284-286°C; IR (KBr) (4000-600 cm^{-1}): ν_{max}: 3330, 2961, 2181, 1661, 1568, 1467, 1332, 1247, 1188, 1045, 995, 764, 732. ^{1}H NMR: (400 MHz, DMSO-d_6) δ 3.72 (s, 4H), 3.88 (d, 2H, 8Hz), 4.105 (q, 3H, J = 12 Hz), 4.66 (s, 1H), 4.82 (s, 1H), 6.62 (s, 2H), 6.93 (m, 2H), 7.13 (d, 2H, J = 8 Hz), 7.17- 7.39 (m, 4H) ppm. ^{13}C NMR: (100 MHz, DMSO-d_6) δ 26.8, 30.4, 33.9, 46.0, 49.1, 52.8, 55.3, 58.2, 115.2, 115.6, 117.4, 120.7, 121.8, 123.0, 123.4, 123.6, 129.2, 129.4, 129.7, 130.0, 137.3, 140.9, 141.3, 154.7, 157.2, 167.5, 202.2 ppm. HR-MS (ESI) for $C_{27}H_{21}N_5O_2$ m/z calcd.: 448.1729; found: 448.1734 $[M+H]^+$.

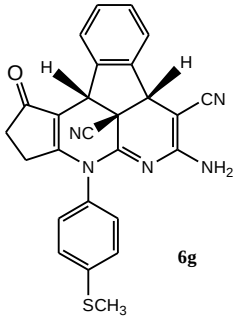

6g

4.7. *6-amino-4-(4-(methylthio)phenyl)-1-oxo-1,2,3,4,7a,11b-hexahydro-4a1H-cyclopenta[b]indeno[1,2,3-de][1,8]naphthyridine-4a1,7-dicarbonitrile (6g).* Yellow solid (75%), > 300°C; IR (KBr) (4000-600 cm^{-1}): ν_{max}: 3328, 2956, 2180, 1633, 1563, 1509, 1467, 1382, 1251, 1188, 997, 767, 647, 610. ^{1}H NMR: (400 MHz, DMSO-d_6) δ 2.38-2.59 (m, 3H), 3.72 (s, 4H), 4.66 (s, 1H), 4.78 (s, 1H), 6.62 (s, 2H), 6.90 (s, 2H), 7.03 (d, 2H, J = 8 Hz), 7.12-7.34 (m, 4H) ppm. ^{13}C NMR: (100 MHz, DMSO-d_6) δ 17.8, 26.5, 34.5, 43.4, 46.6, 49.5, 53.5, 115.2, 117.4, 121.8, 123.0, 123.4, 123.6, 127.9, 129.2, 129.4, 129.7, 130.0, 130.4, 137.3, 140.9, 141.3, 154.1, 157.1, 167.8, 202.1 ppm. HR-MS (ESI) for $C_{26}H_{19}N_5OS$ m/z calcd.: 450.1344; found: 450.1349 $[M+H]^+$.

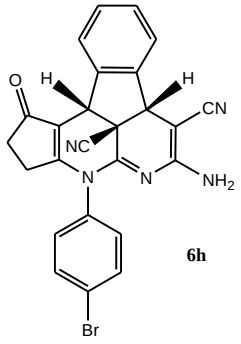

6h

4.8. 6-amino-4-(4-bromophenyl)-1-oxo-1,2,3,4,7a,11b-hexahydro-4a1H-cyclopenta[b]indeno[1,2,3-de][1,8]naphthyridine-4a1,7-dicarbonitrile (6h). Yellow solid (74%), > 300°C; IR (KBr) (4000-600 cm^{-1}): ν_{max}: 3335, 2963, 2176, 1659, 1629, 1568, 1504 1379, 1246, 1189, 991, 842, 739. **^{1}H NMR:** (400 MHz, DMSO-d_6) δ 2.46 (s, 4H), 4.93 (s, 1H), 5.08 (s, 1H), 6.49 (s, 2H), 6.90 (s, 2H), 7.03 (d, 2H, J = 8 Hz), 7.12-7.34 (m, 4H) ppm. **^{13}C NMR:** (100 MHz, DMSO-d_6) δ 24.6, 32.0, 46.0, 49.2, 52.9, 57.0, 115.2, 117.4, 121.8, 123.4, 123.6, 127.9, 129.2, 129.4, 129.7, 130.0, 130.4, 130.6, 137.3, 140.9, 141.3, 157.2, 159.8, 170.5, 204.5 ppm. HR-MS (ESI) for $C_{25}H_{16}BrN_5O$ m/z calcd.: 483.0518; found: 483.0512 $[M+H]^+$.

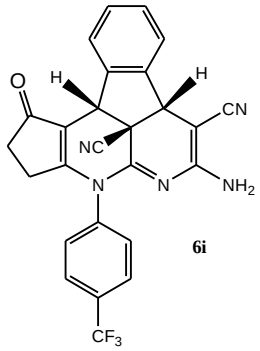

6i

4.9. 6-amino-1-oxo-4-(4-trifluoromethyl)phenyl)-1,2,3,4,7a,11b-hexahydro-4a1H-cyclopenta[b]indeno[1,2,3-de][1,8]naphthyridine-4a1,7-dicarbonitrile (6i). Yellow solid (72%), 284-286°C; IR (KBr) (4000-600 cm^{-1}): ν_{max}: 3339, 2960, 2174, 1621, 1593, 1457, 1385, 1275, 1128, 998, 732, 616. ^{1}H NMR: (400 MHz, DMSO-d_6) δ 3.72 (s, 4H), 4.66 (s, 1H), 4.78 (s, 1H), 6.40 (s, 2H), 6.66 (s, 2H), 6.74-6.81 (m, 2H), 7.12-7.34 (m, 4H) ppm. ^{13}C NMR: (100 MHz, DMSO-d_6) δ 24.6, 32.0, 46.0, 49.2, 52.9, 57.0, 97.1, 115.2, 117.4, 121.8, 123.4, 123.6, 127.9, 129.2, 129.4, 129.7, 130.0, 130.4, 130.6, 137.3, 140.9, 141.3, 157.2, 159.8, 170.5, 204.5 ppm. HR-MS (ESI) for $C_{26}H_{16}F_3N_5O$ m/z calcd.: 472.1340; found: 472.1352 $[M+H]^+$.

5. ^{1}H NMR and ^{13}C NMR Spectra of all compounds

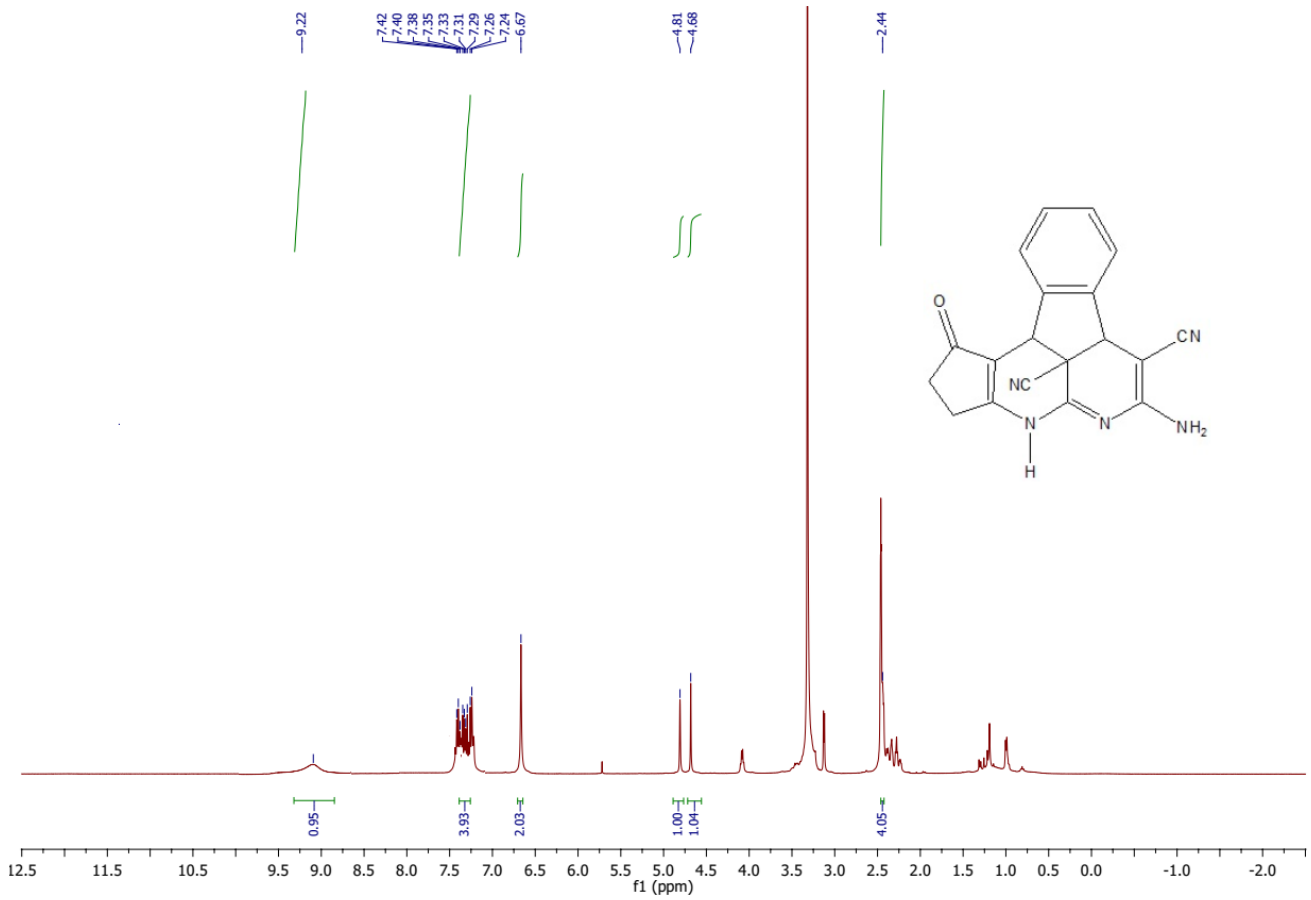

Figure S1: ^{1}H NMR of compound **6a**

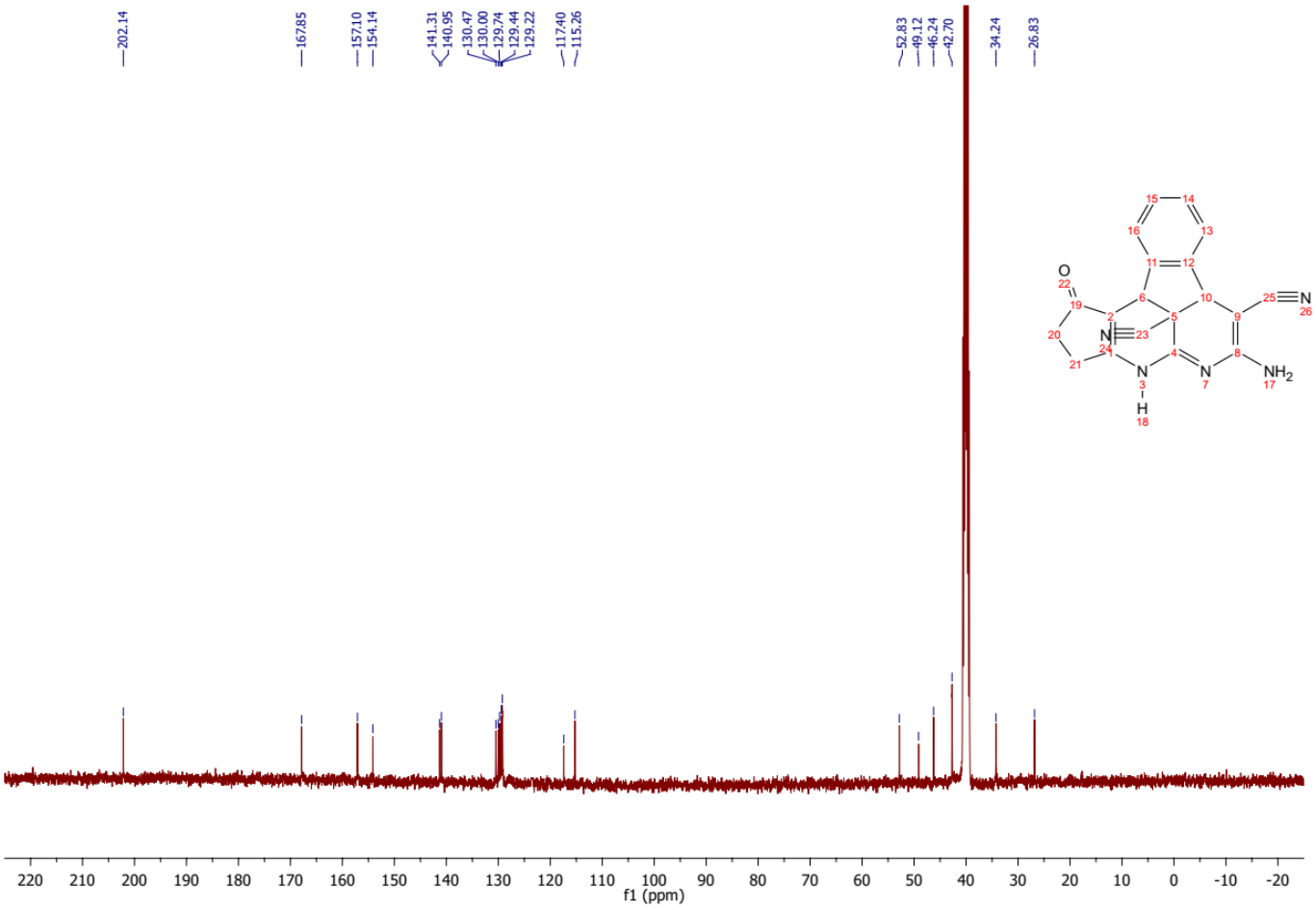

Figure S2: ^{13}C NMR of compound **6a**

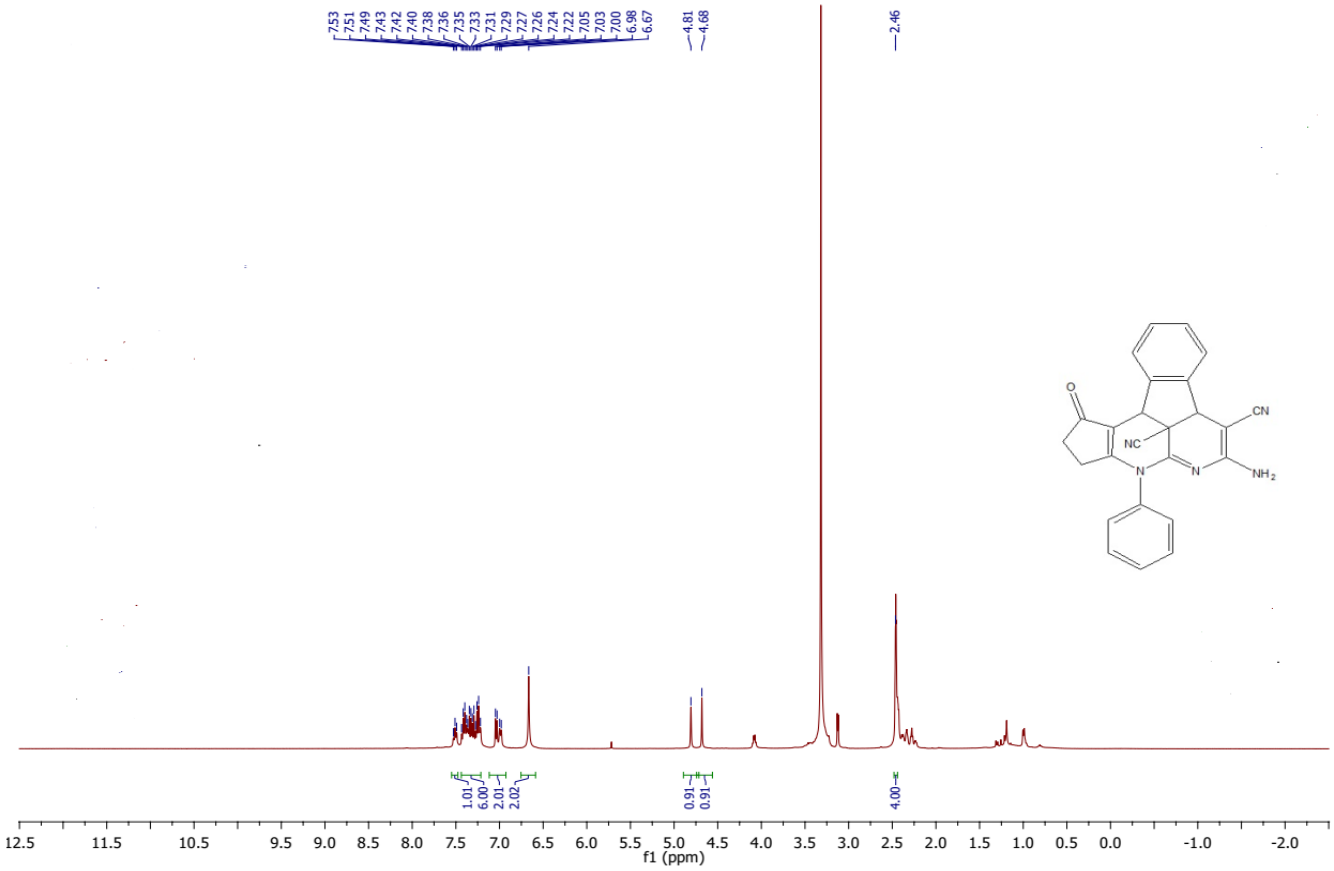

Figure S3: ^{1}H NMR of compound **6b**

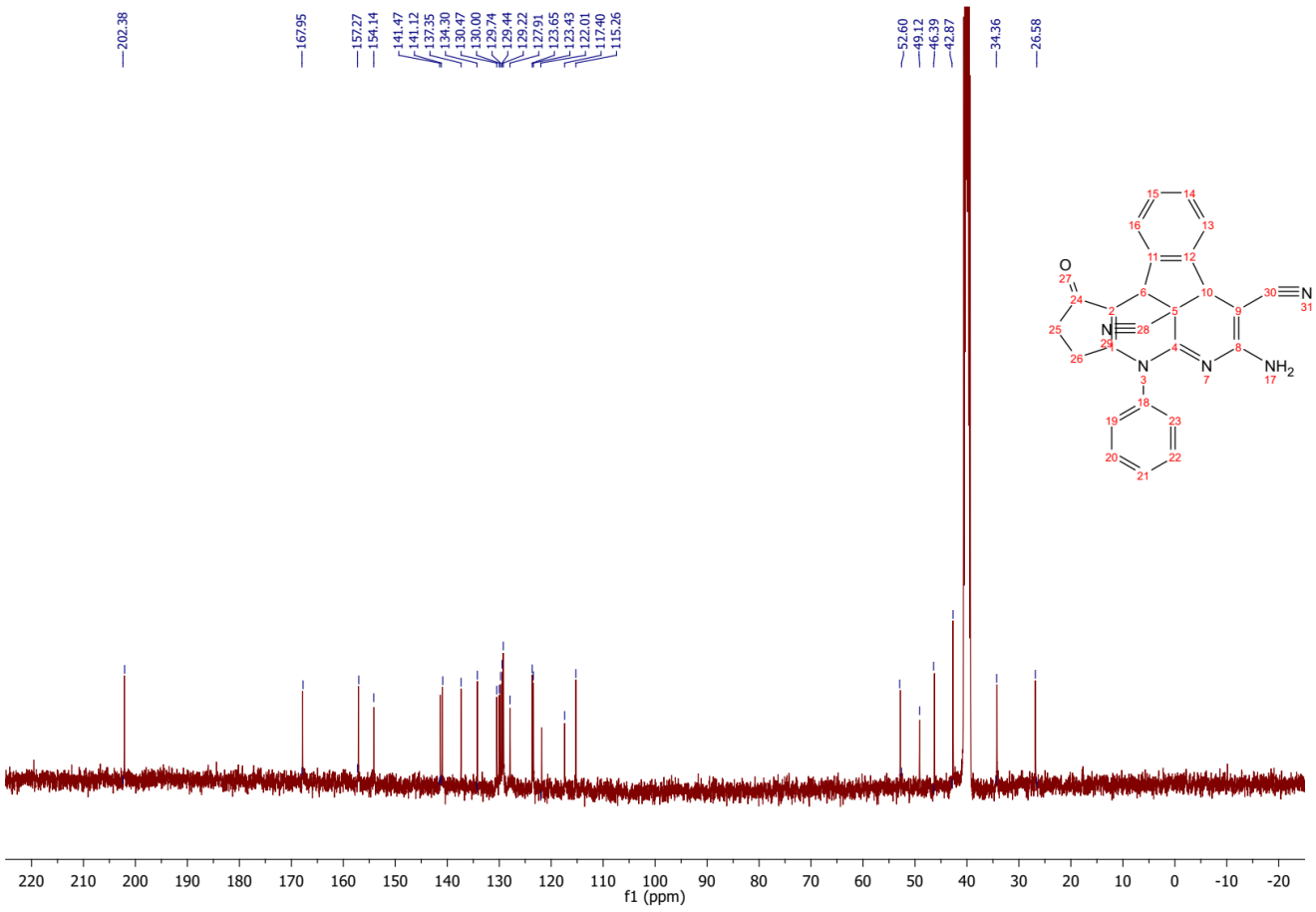

Figure S4: ^{13}C NMR of compound **6b**

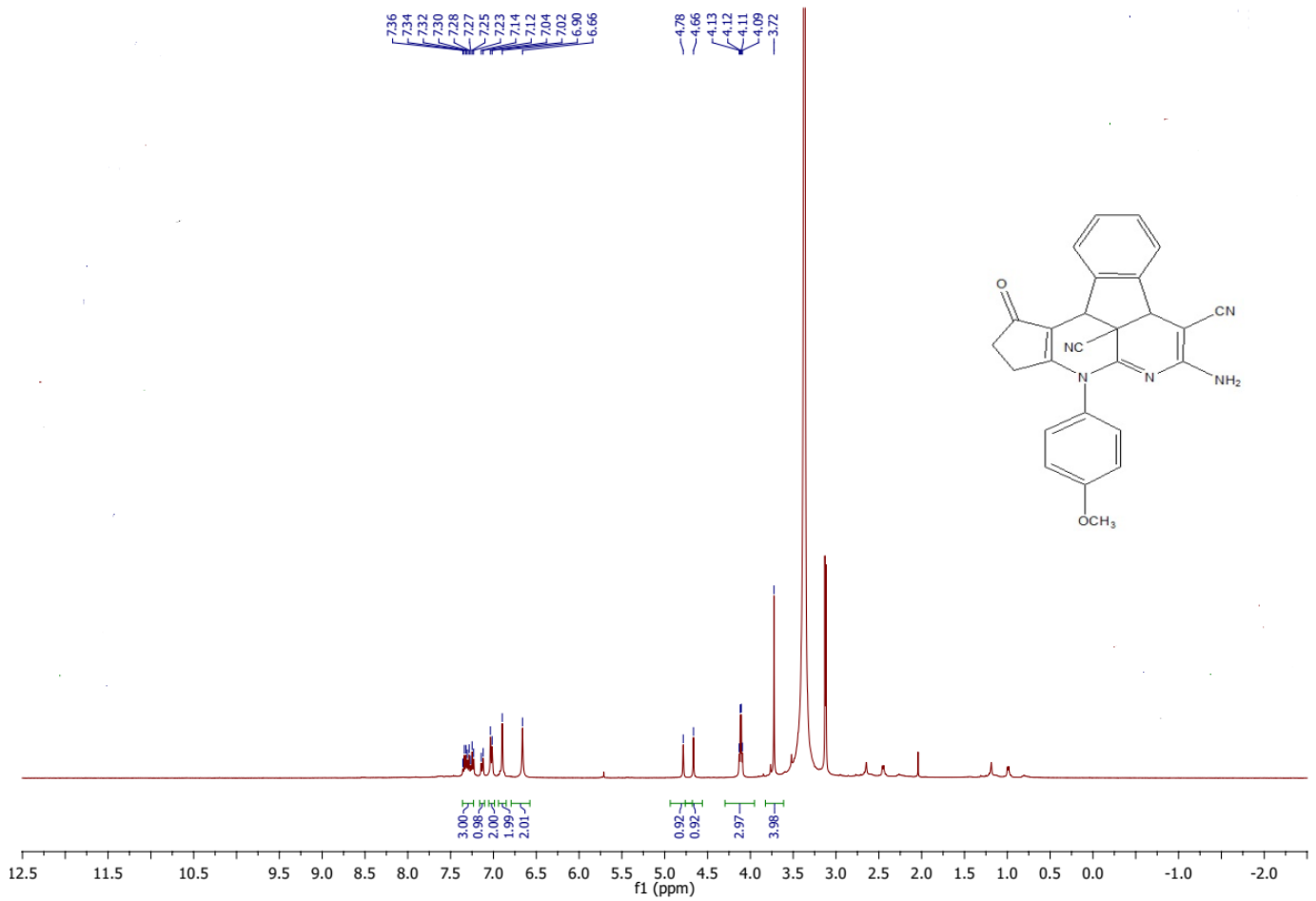

Figure S5: ^{1}H NMR of compound **6c**

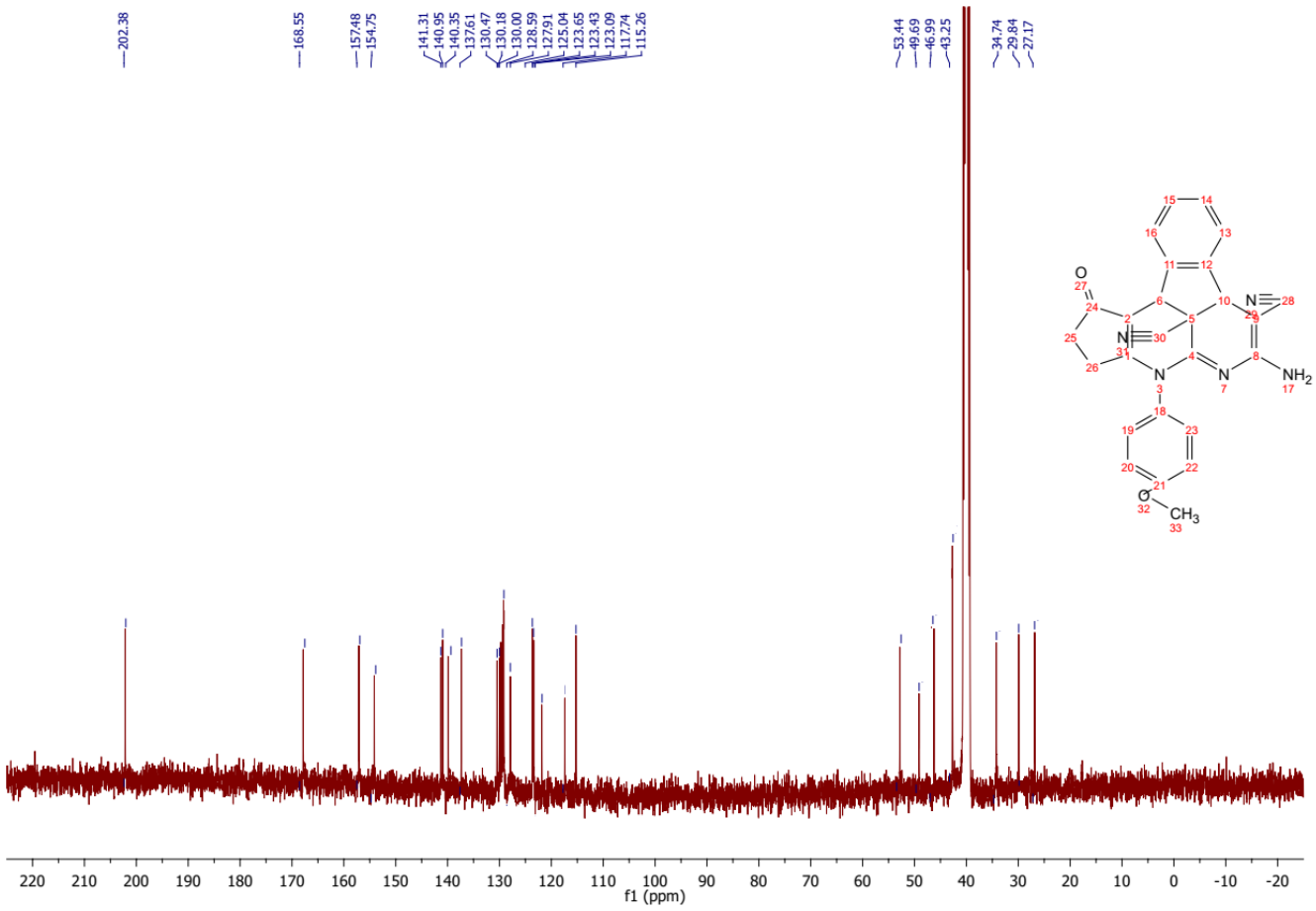

Figure S6: ^{13}C NMR of compound **6c**

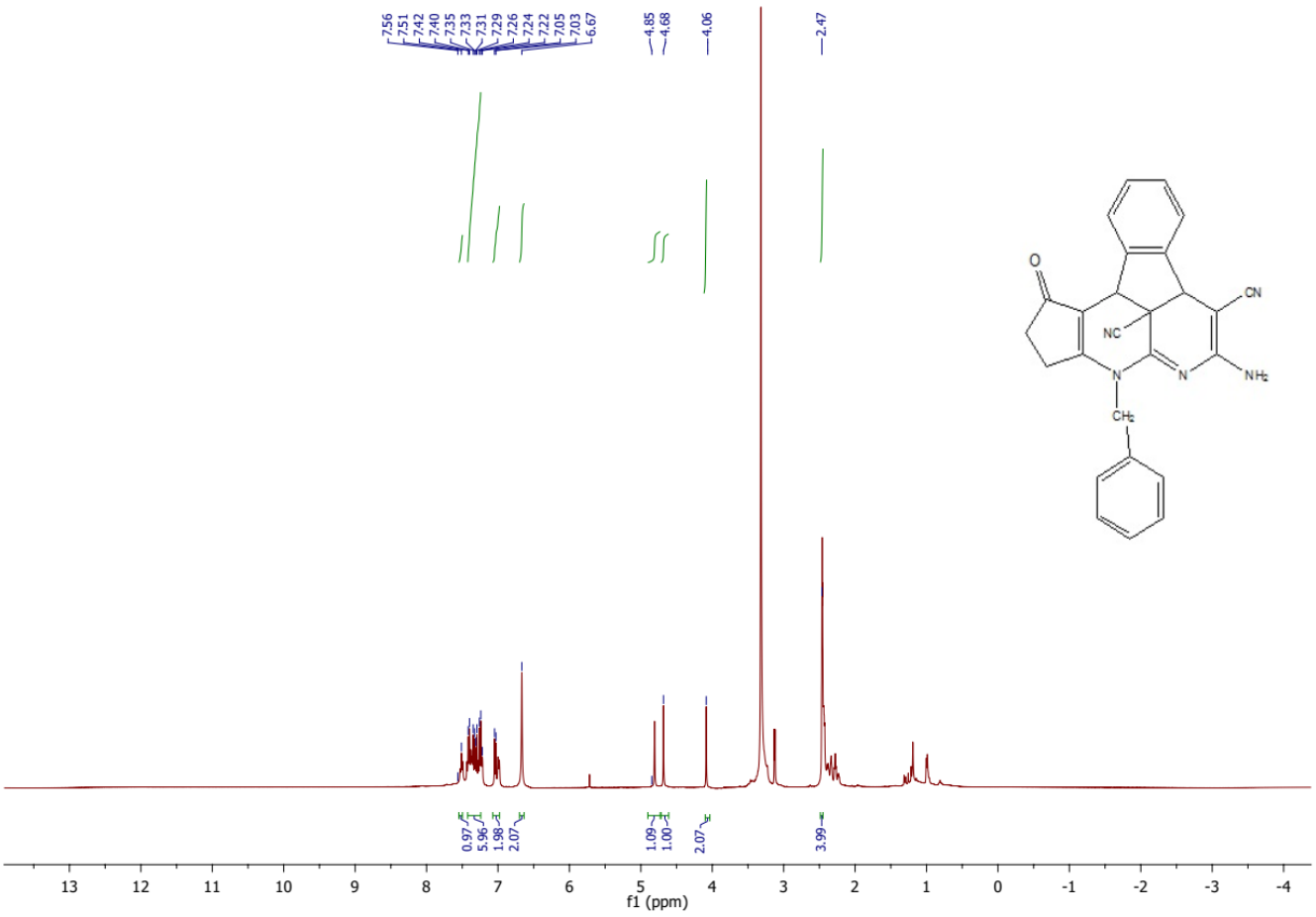

Figure S7: ^{1}H NMR of compound **6d**

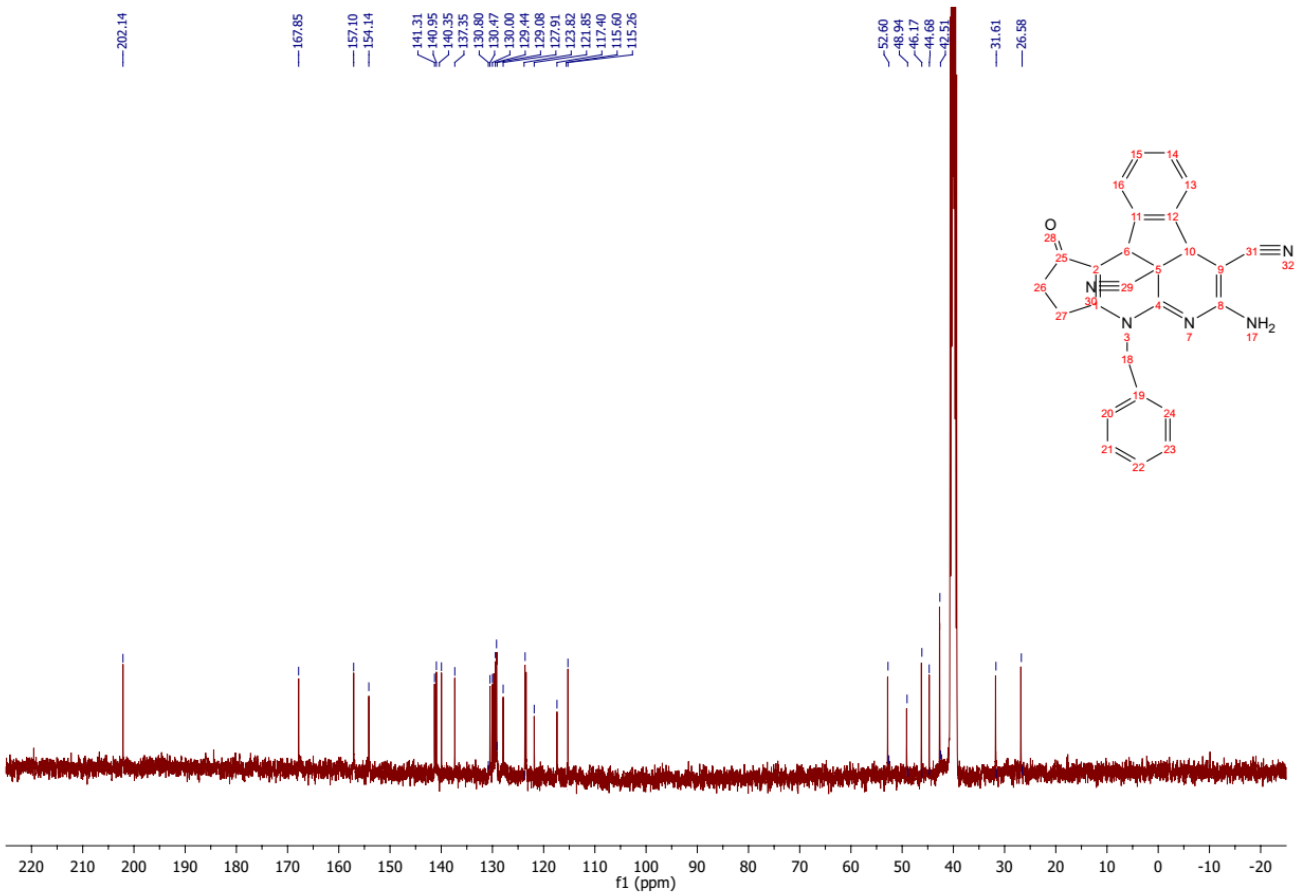

Figure S8: ^{13}C NMR of compound **6d**

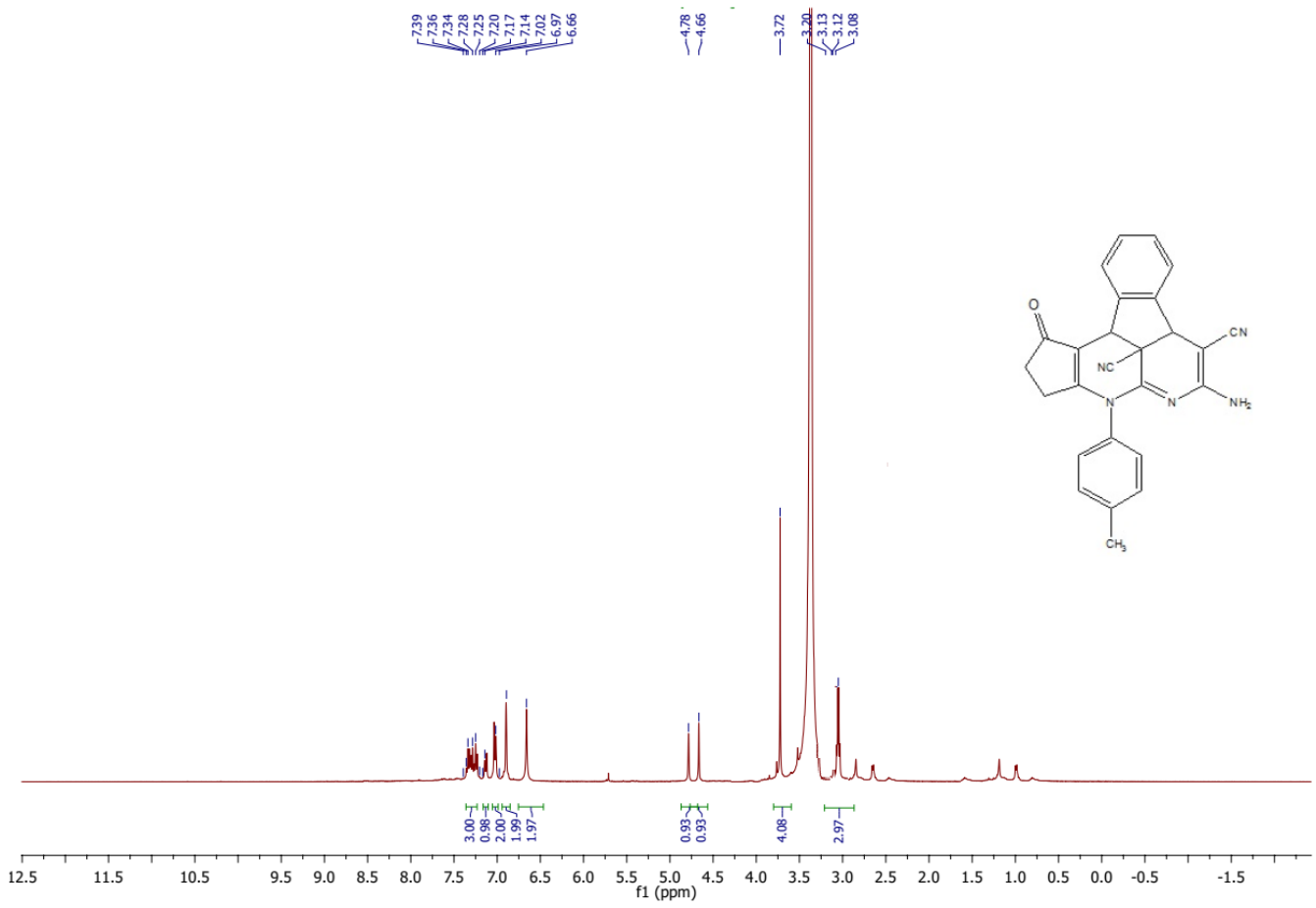

Figure S9: ^{1}H NMR of compound **6e**

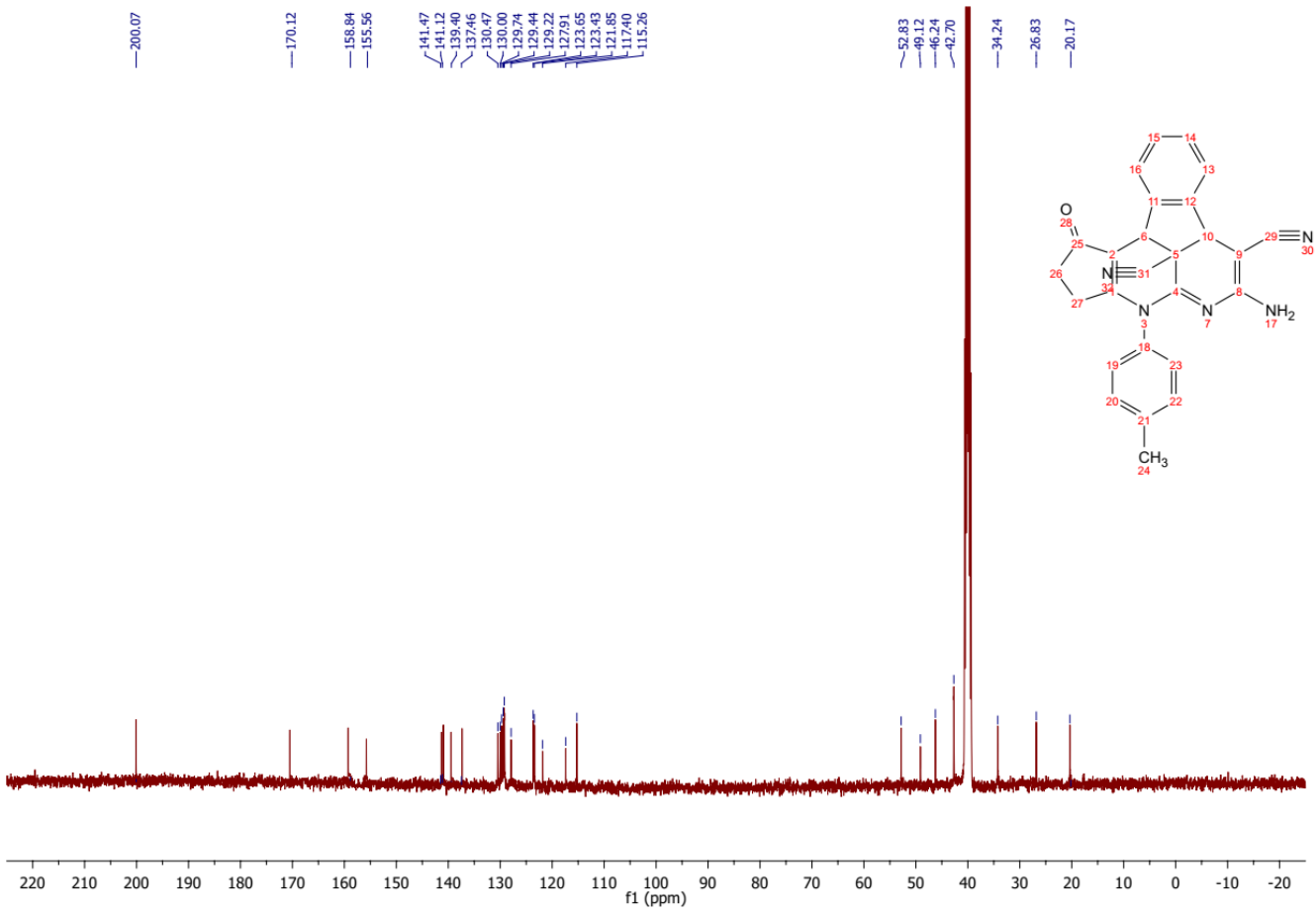

Figure S10: ^{13}C NMR of compound **6e**

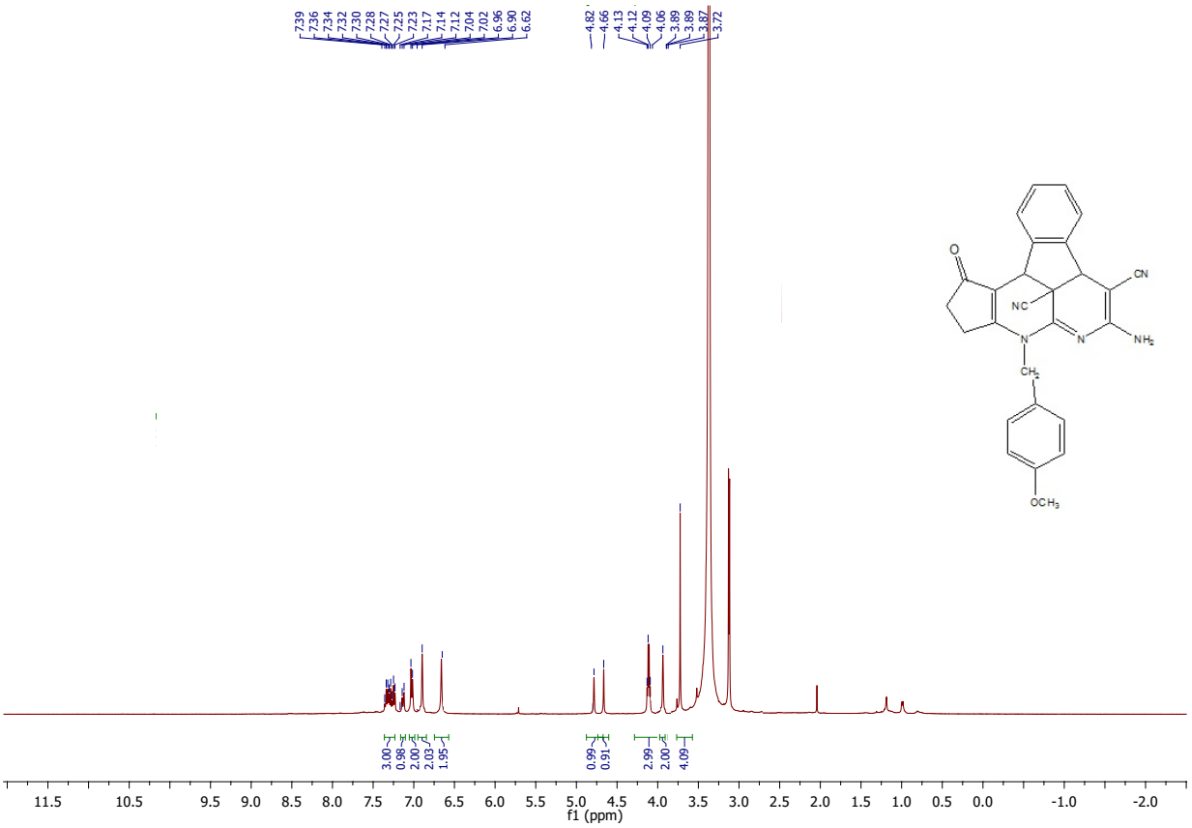

Figure S11: ^{1}H NMR of compound **6f**

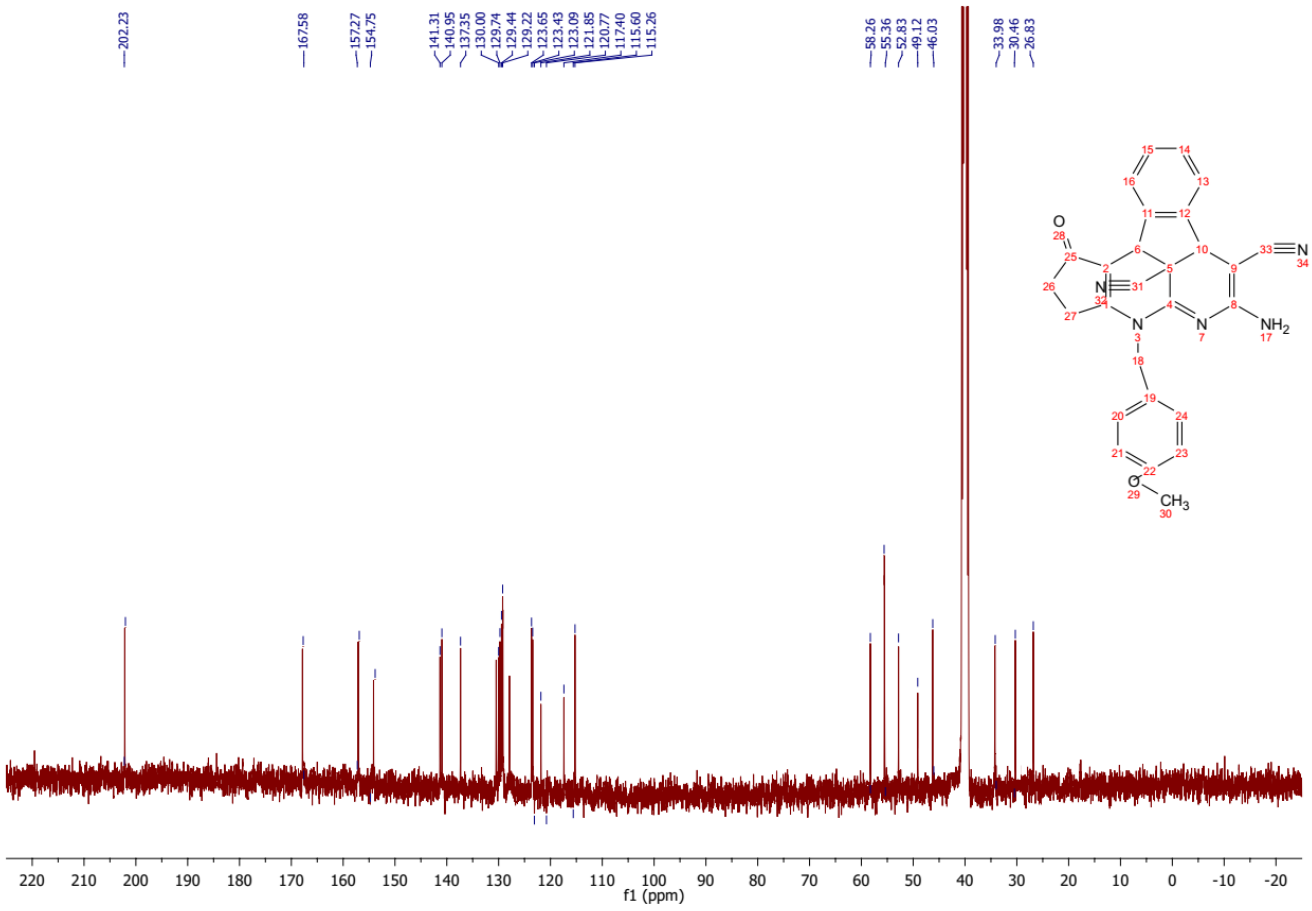

Figure S12: ^{13}C NMR of compound **6f**

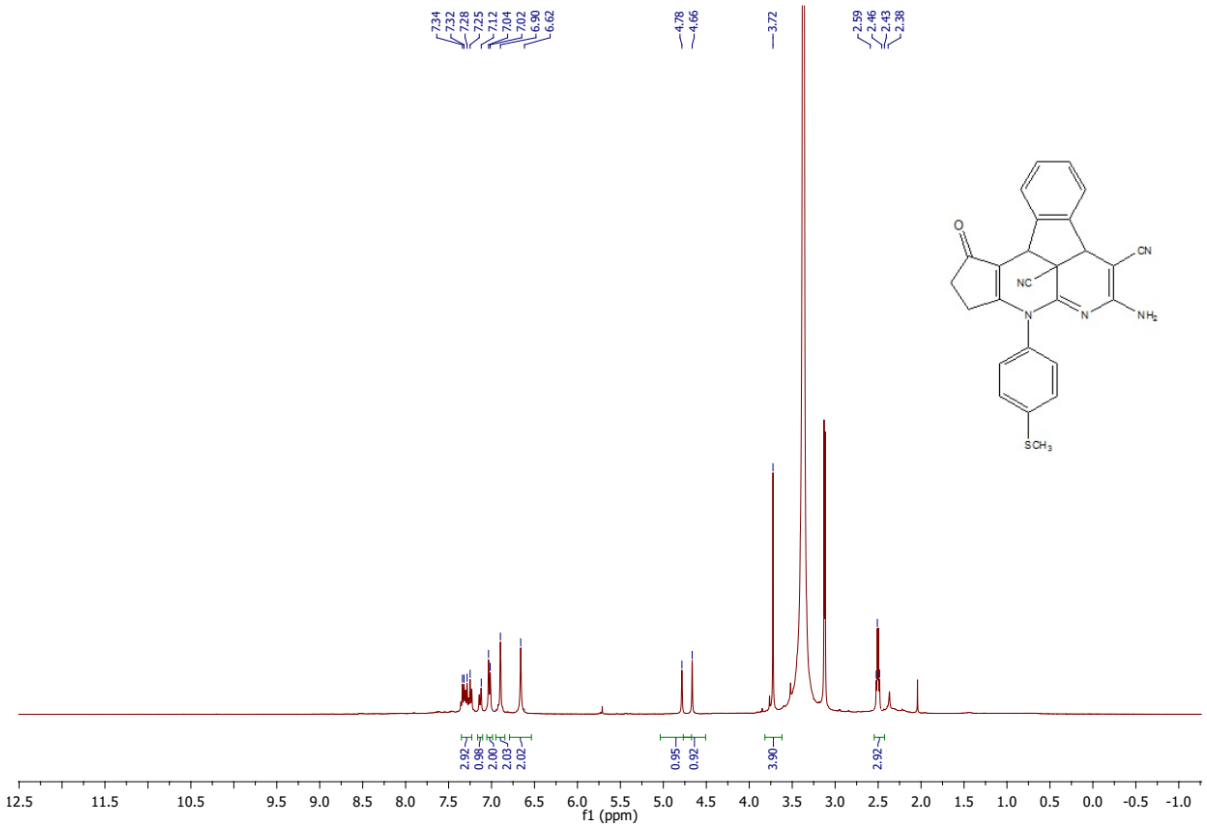

Figure S13: ^{1}H NMR of compound **6g**

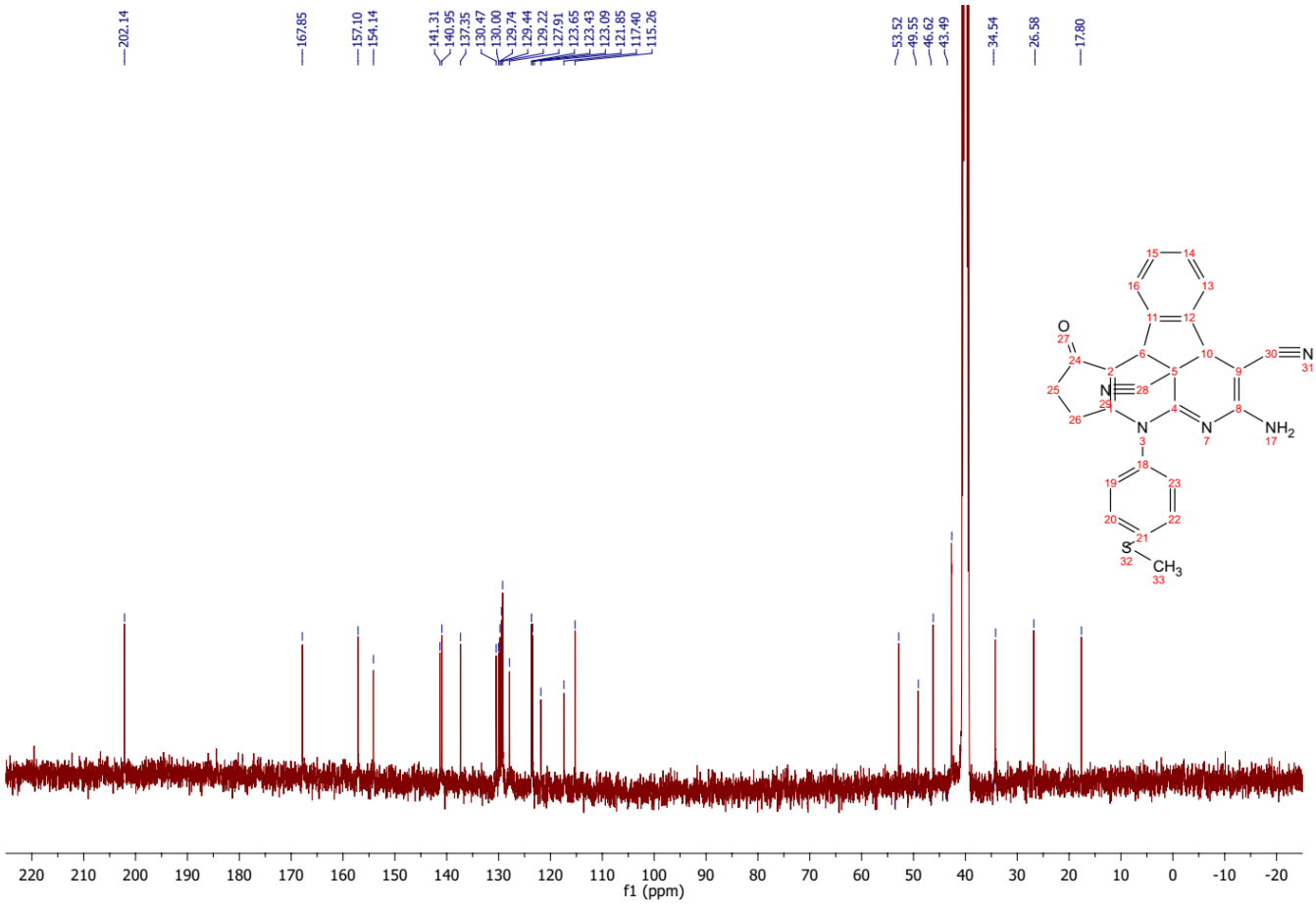

Figure S14: ^{13}C NMR of compound **6g**

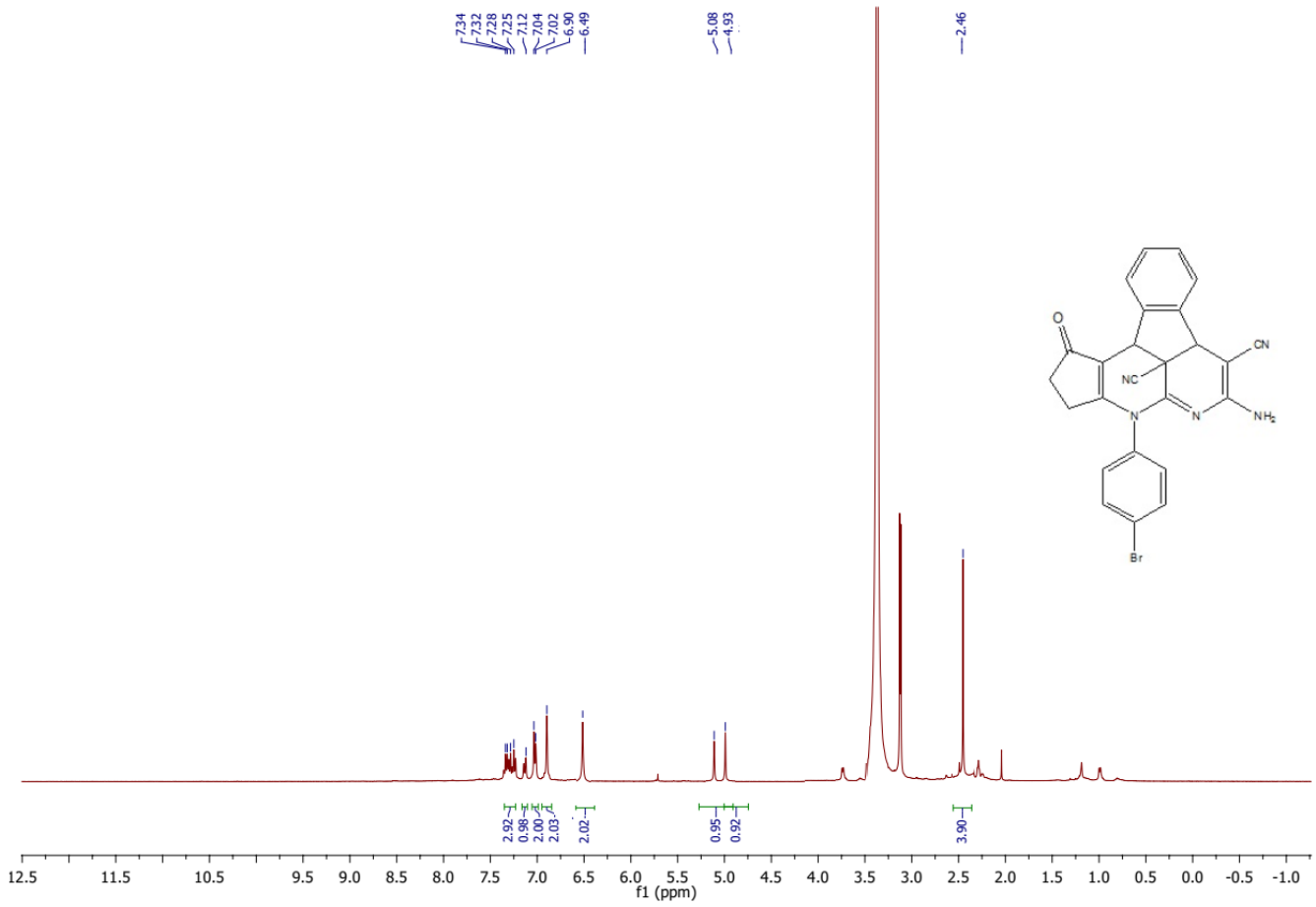

Figure S15: ^{1}H NMR of compound **6h**

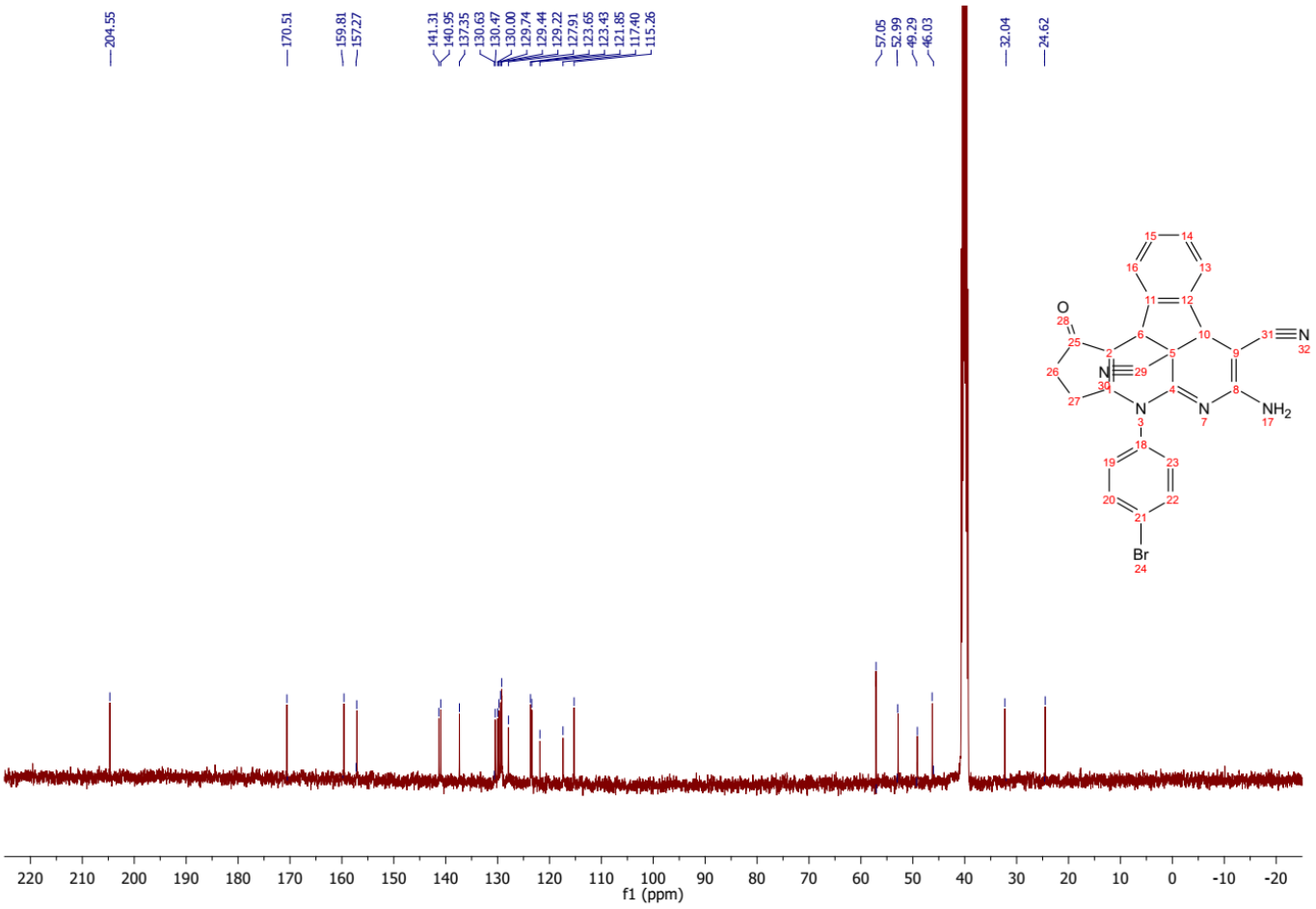

Figure S16: ^{13}C NMR of compound **6h**

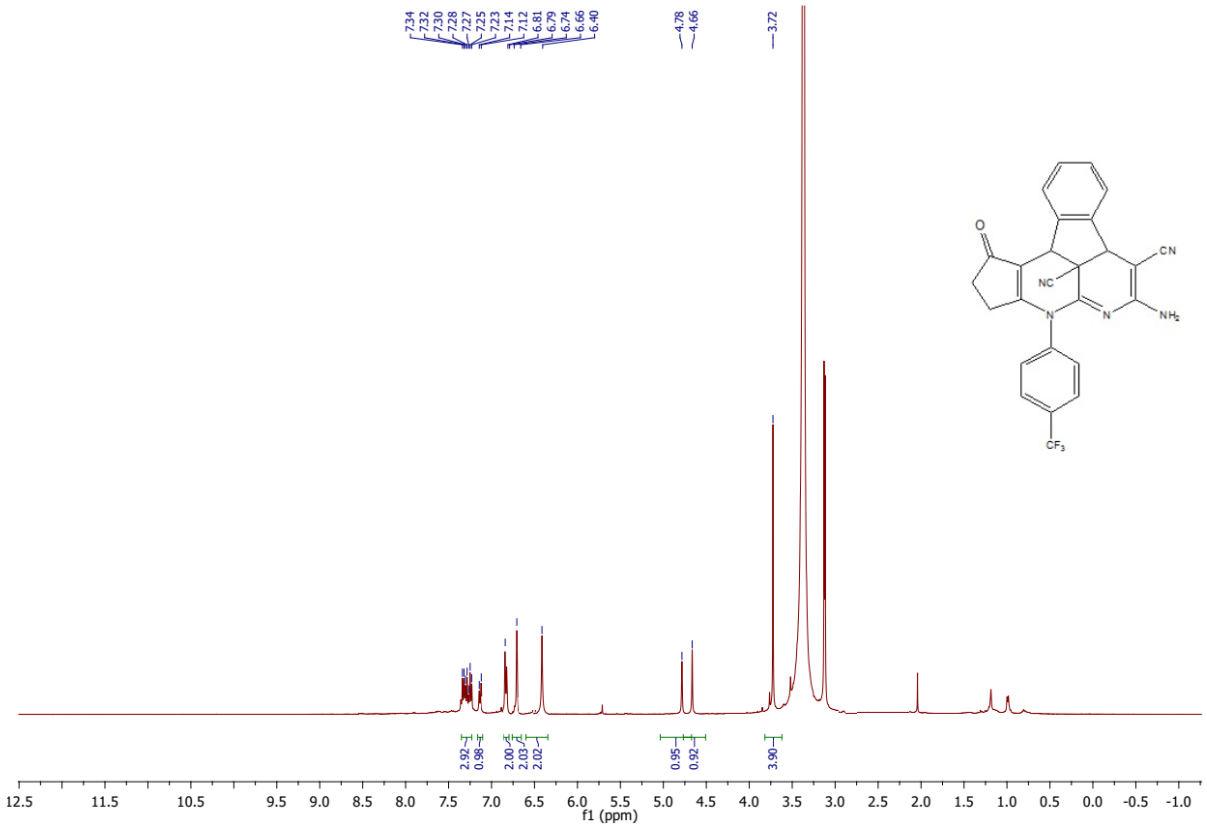

Figure S17: ^{1}H NMR of compound **6i**

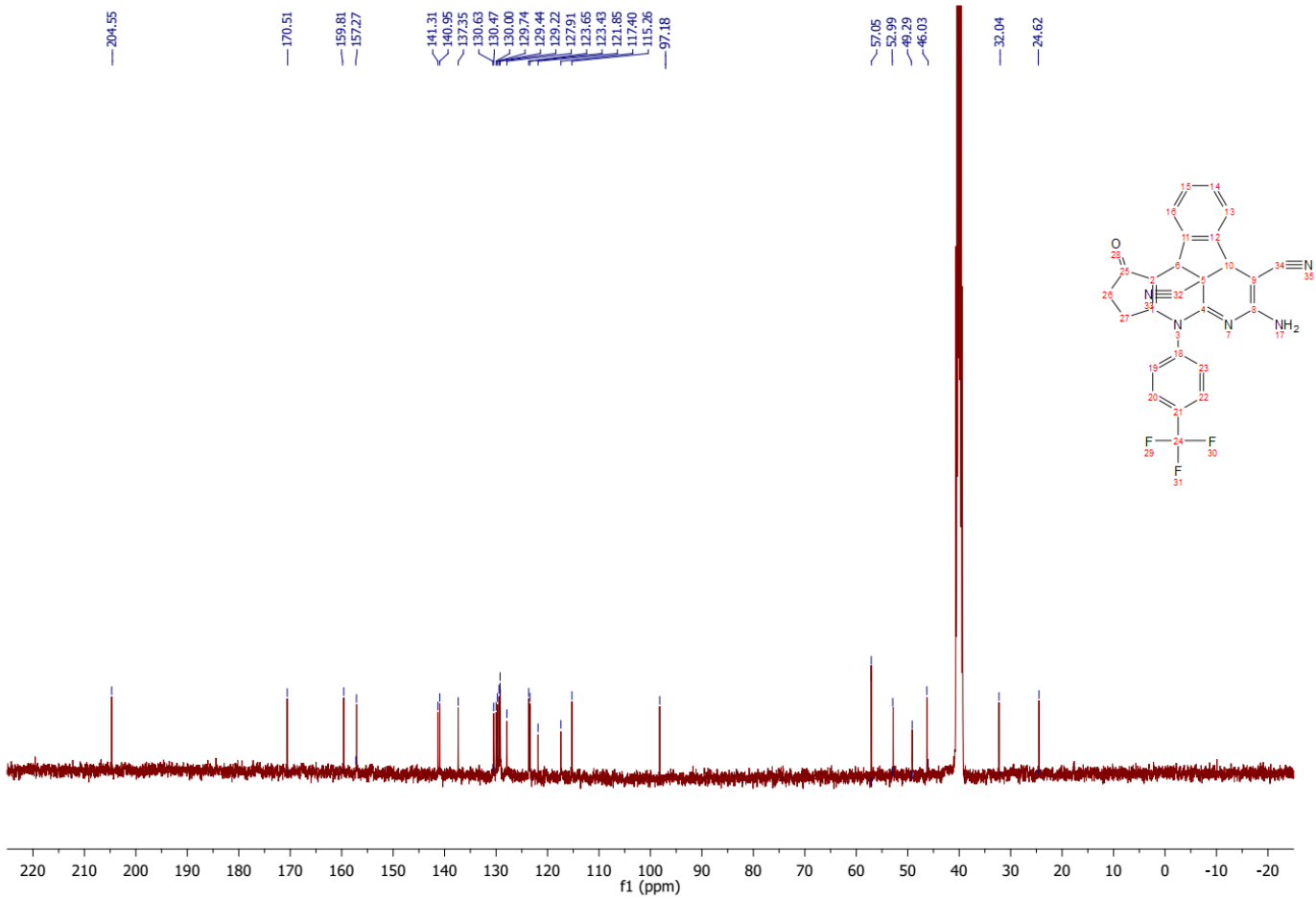

Figure S18: ^{13}C NMR of compound **6i**

6. The 2D and 3D binding interactions of Vosaroxin and all synthesized compounds (6a-i) against human topoisomerase IIβ (PDB ID: 3QX3)

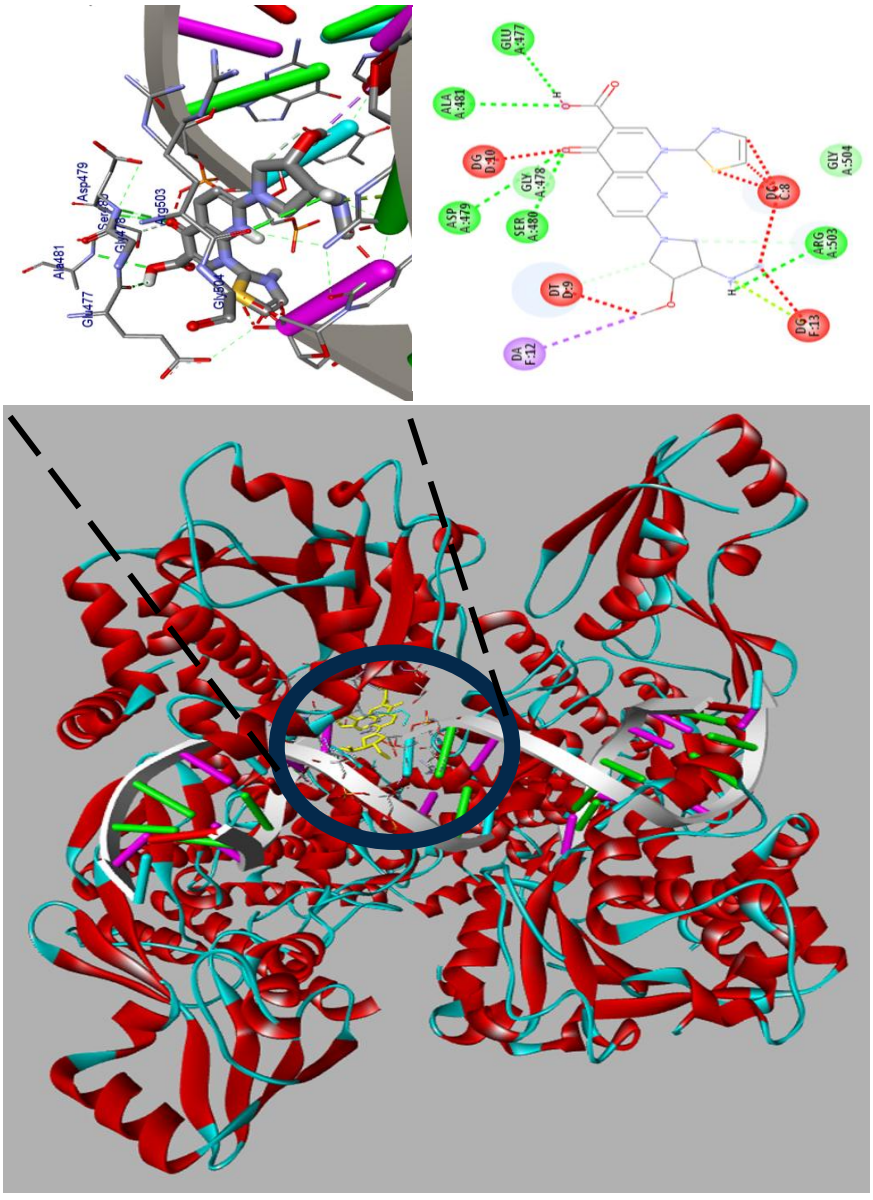

Figure S19: The 2D and 3D binding interactions of compound **Vosaroxin** against human topoisomerase IIβ (PDB ID: 3QX3). 3D Ribbon model shows the binding pocket structure of human topoisomerase IIβ with **Vosaroxin**. Hydrogen bond between compounds and amino acids are shown as green dash lines, hydrophobic interactions are shown as pink lines.

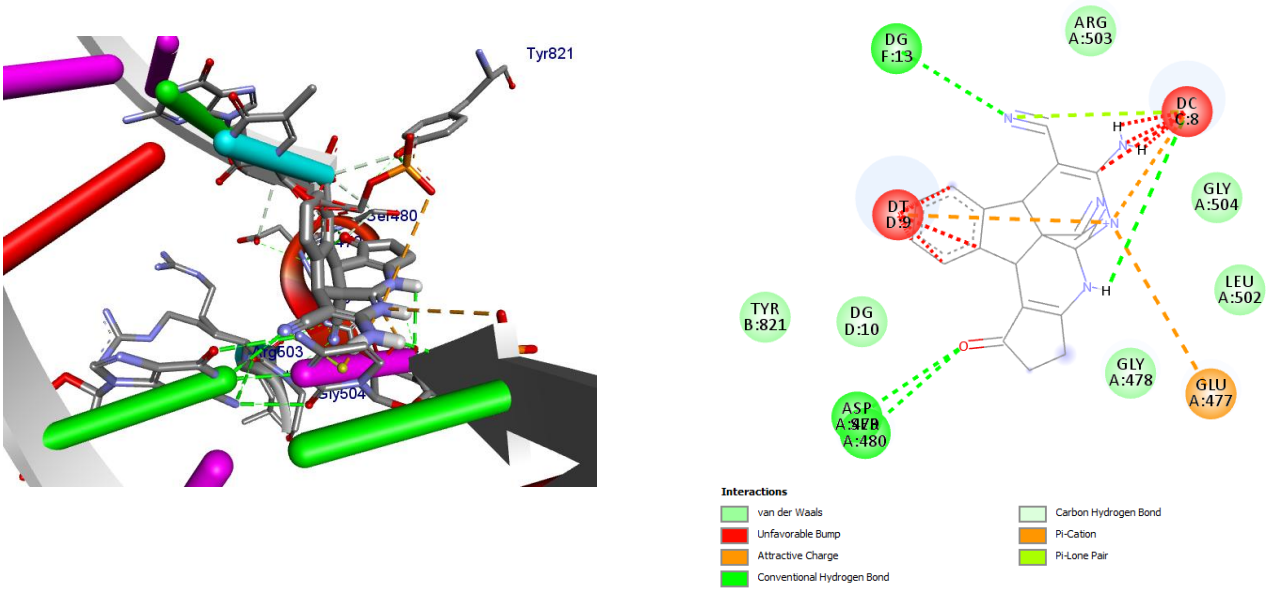

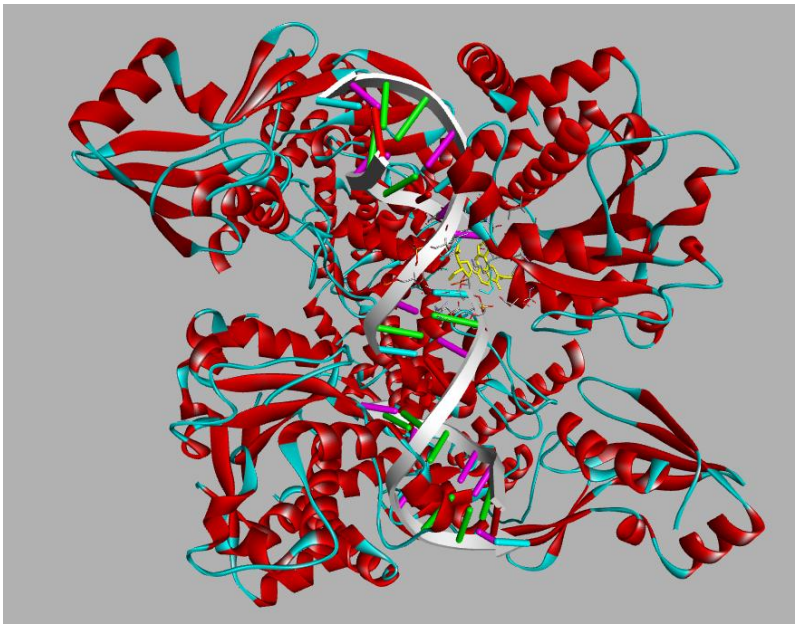

Figure S20: The 2D and 3D binding interactions of compound **6a** against human topoisomerase IIβ (PDB ID: 3QX3). 3D Ribbon model shows the binding pocket structure of human topoisomerase IIβ with compound **6a**. Hydrogen bond between compounds and amino acids are shown as green dash lines, hydrophobic interactions are shown as pink lines.

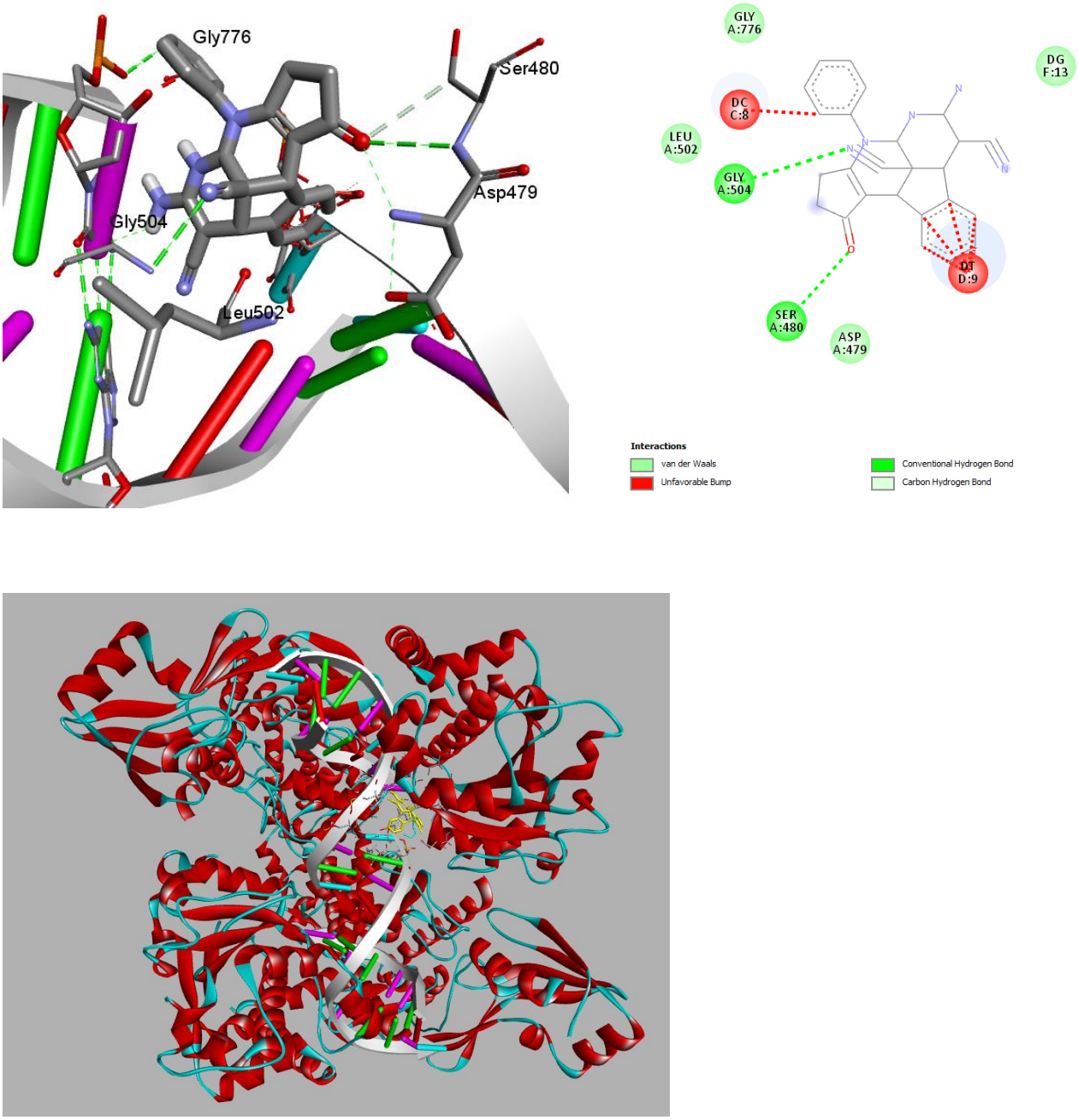

Figure S21: The 2D and 3D binding interactions of compound **6b** against human topoisomerase IIβ (PDB ID: 3QX3). 3D Ribbon model shows the binding pocket structure of human topoisomerase IIβ with compound **6b**. Hydrogen bond between compounds and amino acids are shown as green dash lines, hydrophobic interactions are shown as pink lines.

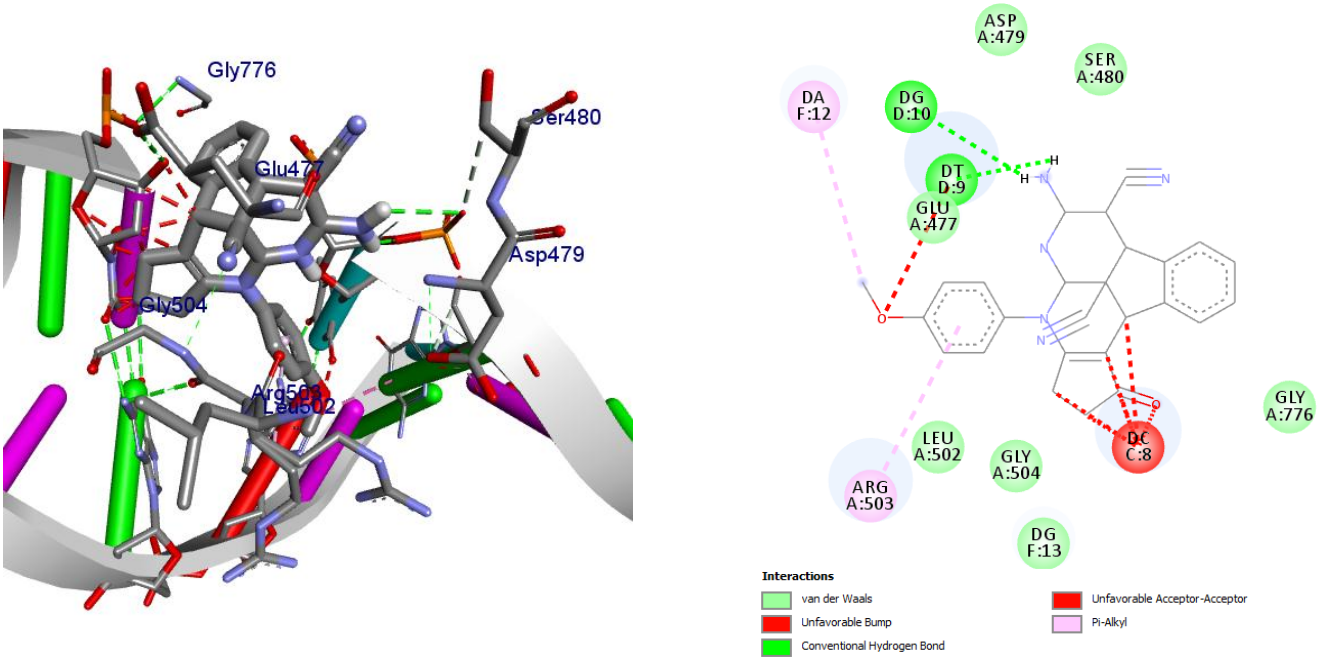

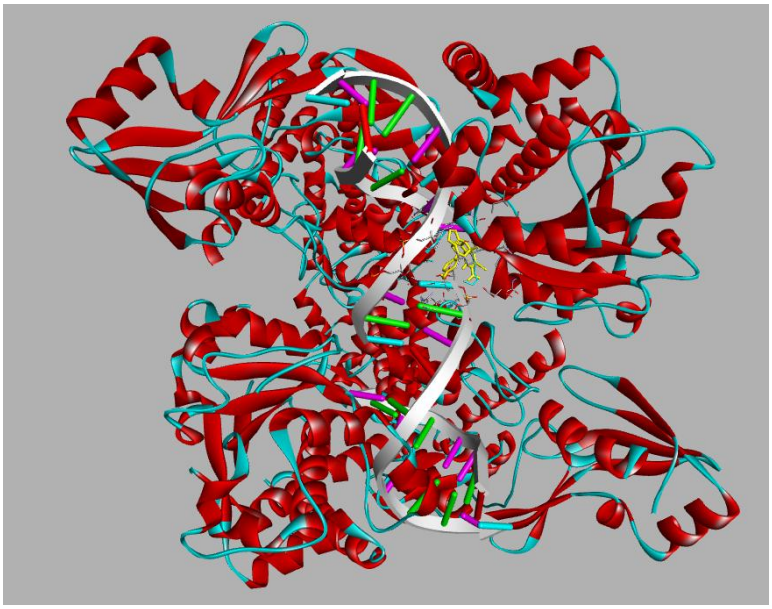

Figure S22: The 2D and 3D binding interactions of compound **6c** against human topoisomerase IIβ (PDB ID: 3QX3). 3D Ribbon model shows the binding pocket structure of human topoisomerase IIβ with compound **6c**. Hydrogen bond between compounds and amino acids are shown as green dash lines, hydrophobic interactions are shown as pink lines.

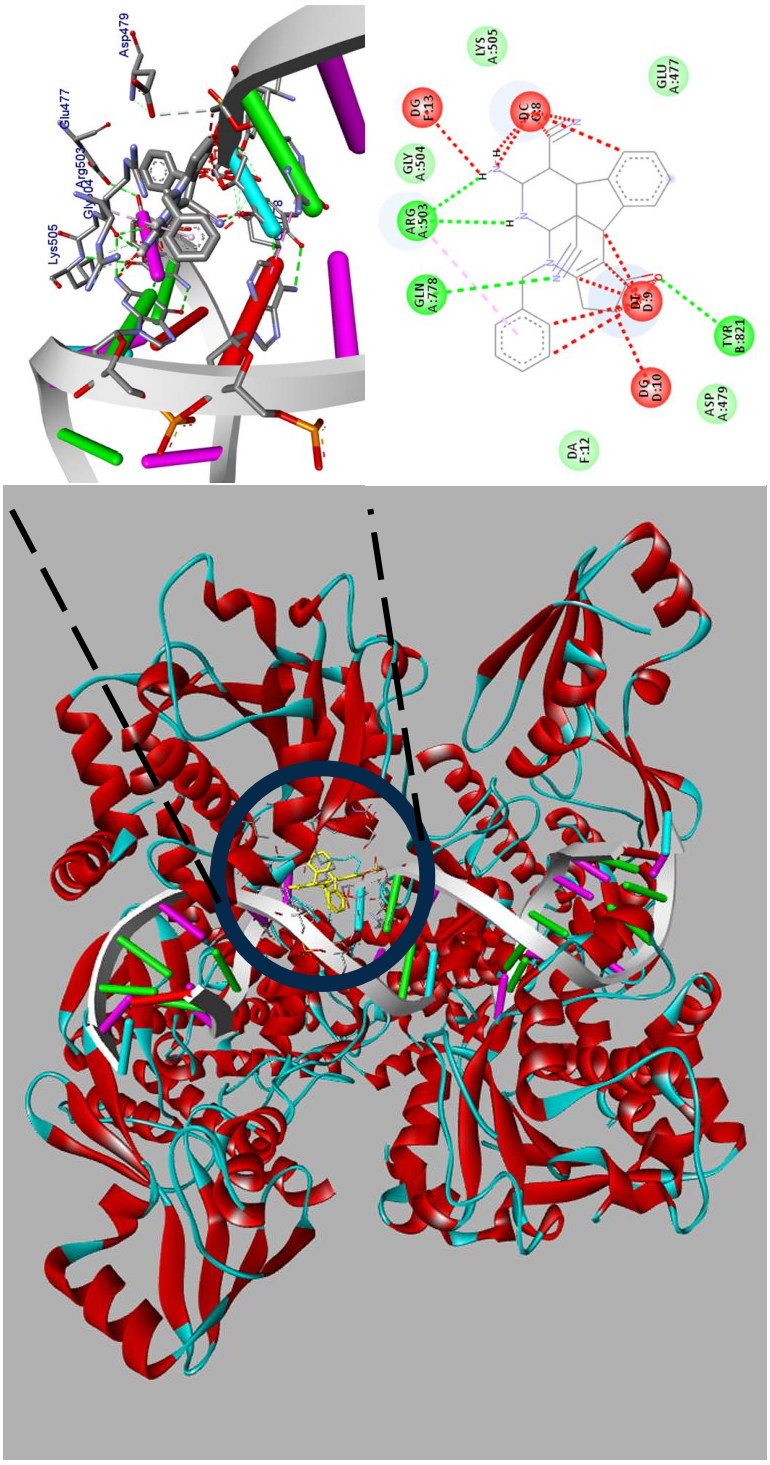

Figure S23: The 2D and 3D binding interactions of compound **6d** against human topoisomerase IIβ (PDB ID: 3QX3). 3D Ribbon model shows the binding pocket structure of human topoisomerase IIβ with compound **6d**. Hydrogen bond between compounds and amino acids are shown as green dash lines, hydrophobic interactions are shown as pink lines.

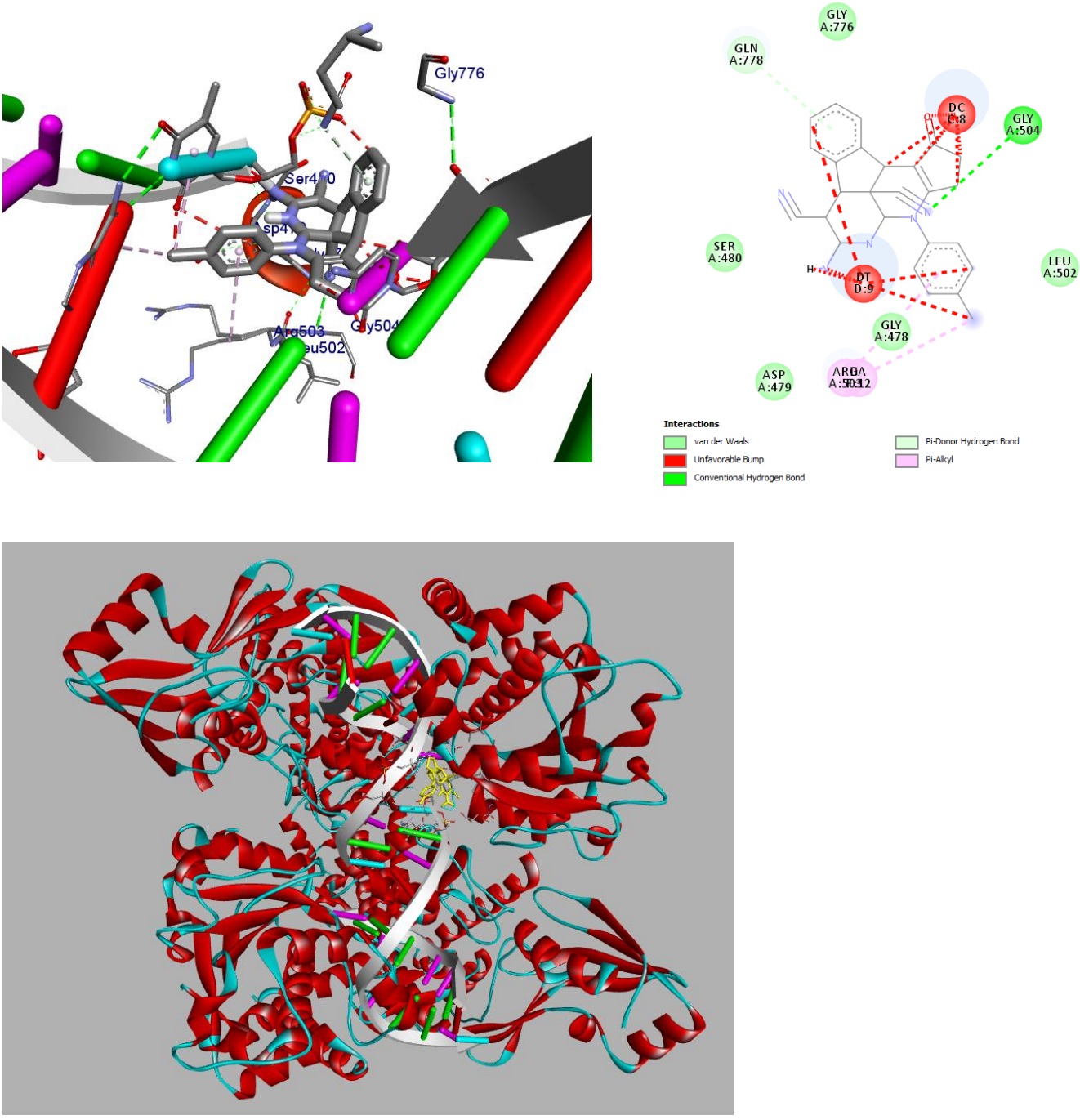

Figure S24: The 2D and 3D binding interactions of compound **6e** against human topoisomerase IIβ (PDB ID: 3QX3). 3D Ribbon model shows the binding pocket structure of human topoisomerase IIβ with compound **6e**. Hydrogen bond between compounds and amino acids are shown as green dash lines, hydrophobic interactions are shown as pink lines.

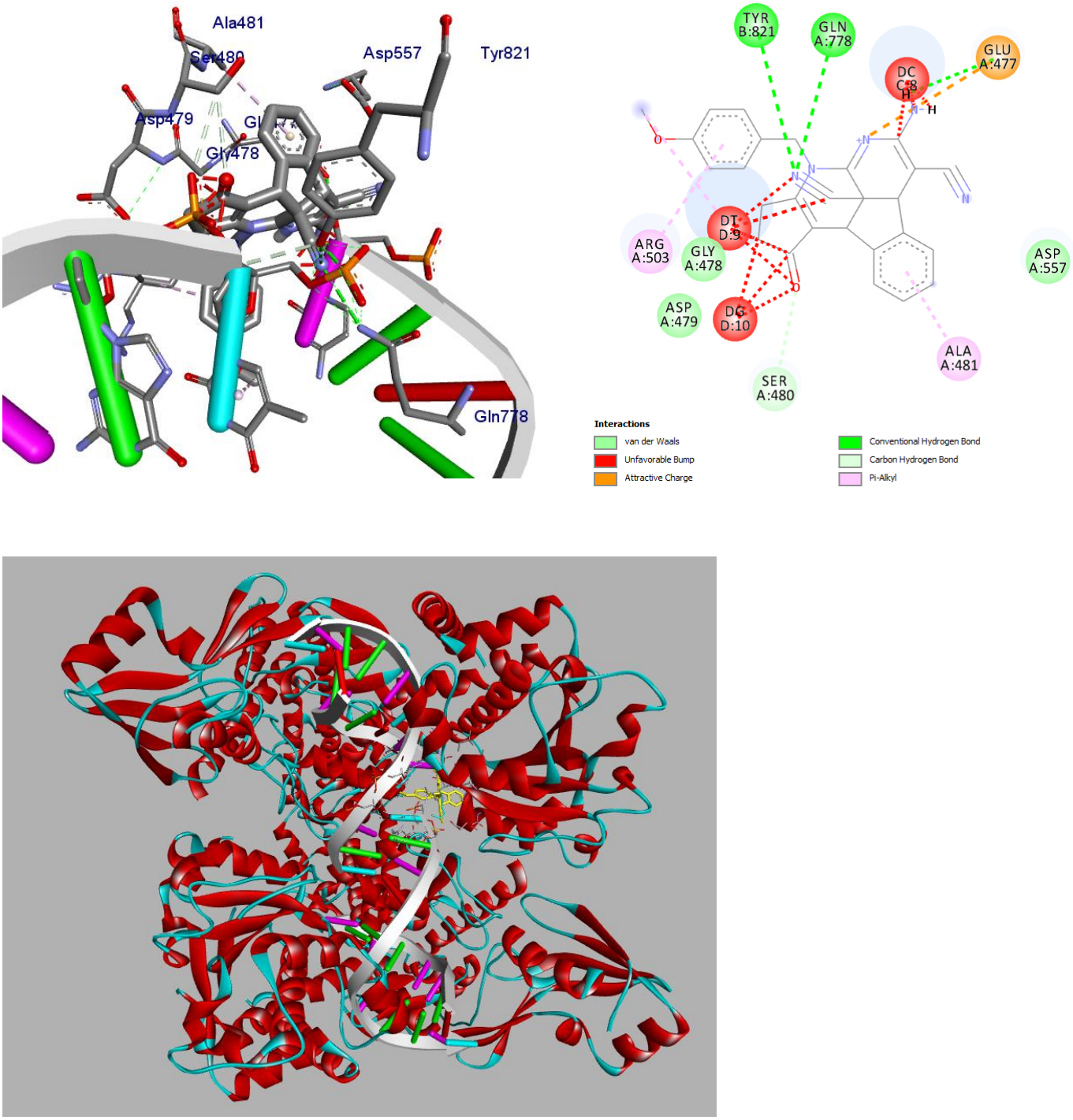

Figure S25: The 2D and 3D binding interactions of compound **6f** against human topoisomerase IIβ (PDB ID: 3QX3). 3D Ribbon model shows the binding pocket structure of human topoisomerase IIβ with compound **6f**. Hydrogen bond between compounds and amino acids are shown as green dash lines, hydrophobic interactions are shown as pink lines.

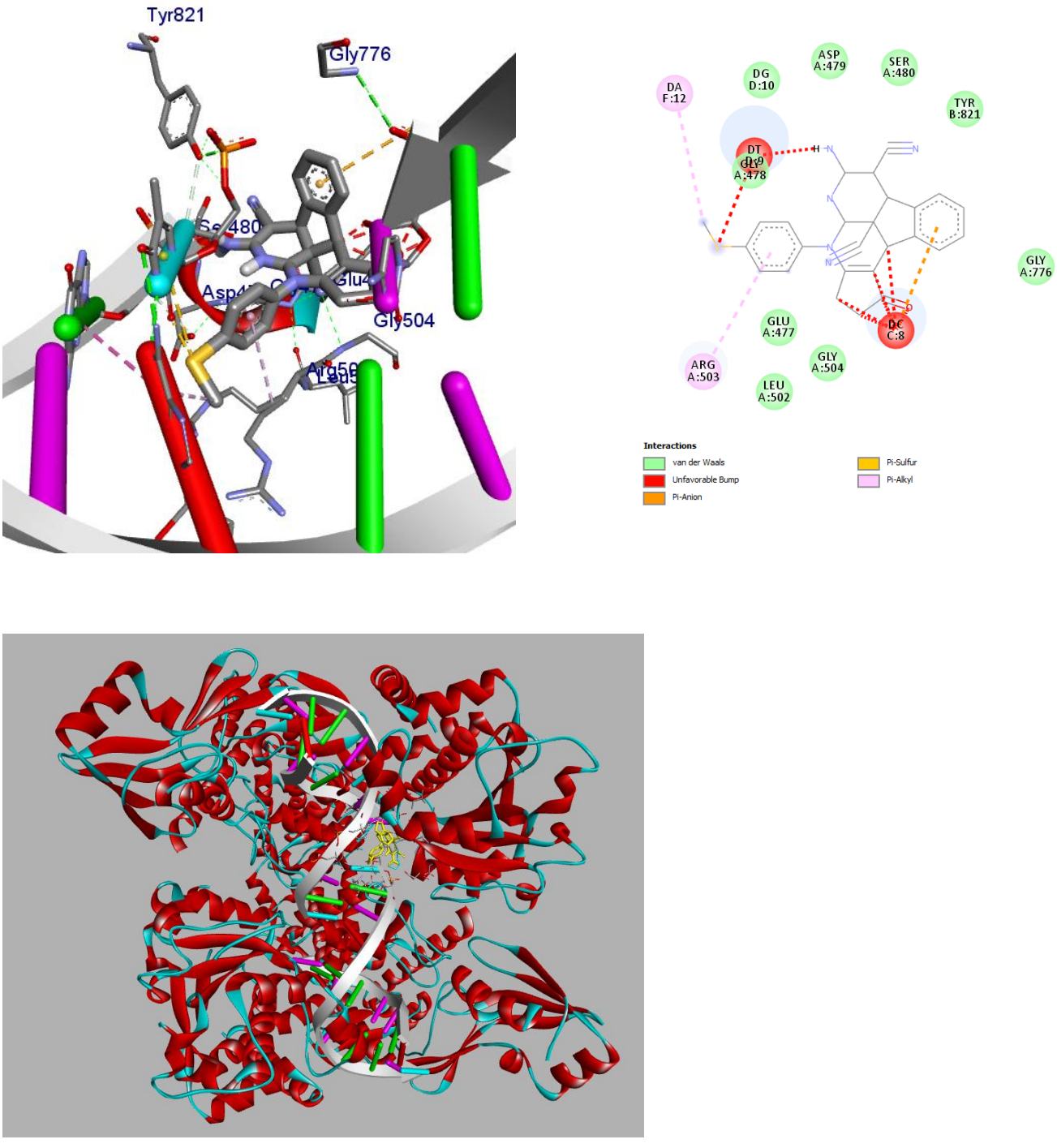

Figure S26: The 2D and 3D binding interactions of compound **6g** against human topoisomerase IIβ (PDB ID: 3QX3). 3D Ribbon model shows the binding pocket structure of human topoisomerase IIβ with compound **6g**. Hydrogen bond between compounds and amino acids are shown as green dash lines, hydrophobic interactions are shown as pink lines.

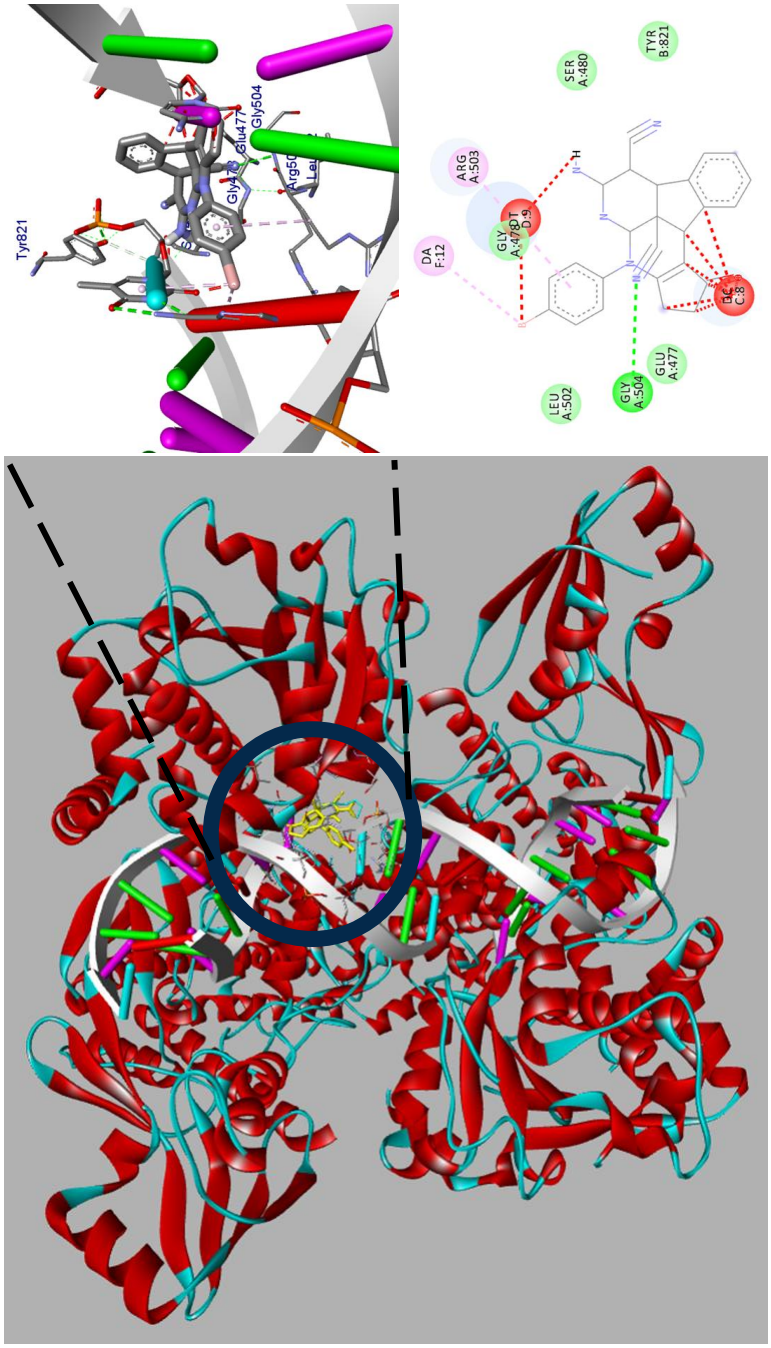

Figure S27: The 2D and 3D binding interactions of compound **6h** against human topoisomerase IIβ (PDB ID: 3QX3). 3D Ribbon model shows the binding pocket structure of human topoisomerase IIβ with compound **6h**. Hydrogen bond between compounds and amino acids are shown as green dash lines, hydrophobic interactions are shown as pink lines.

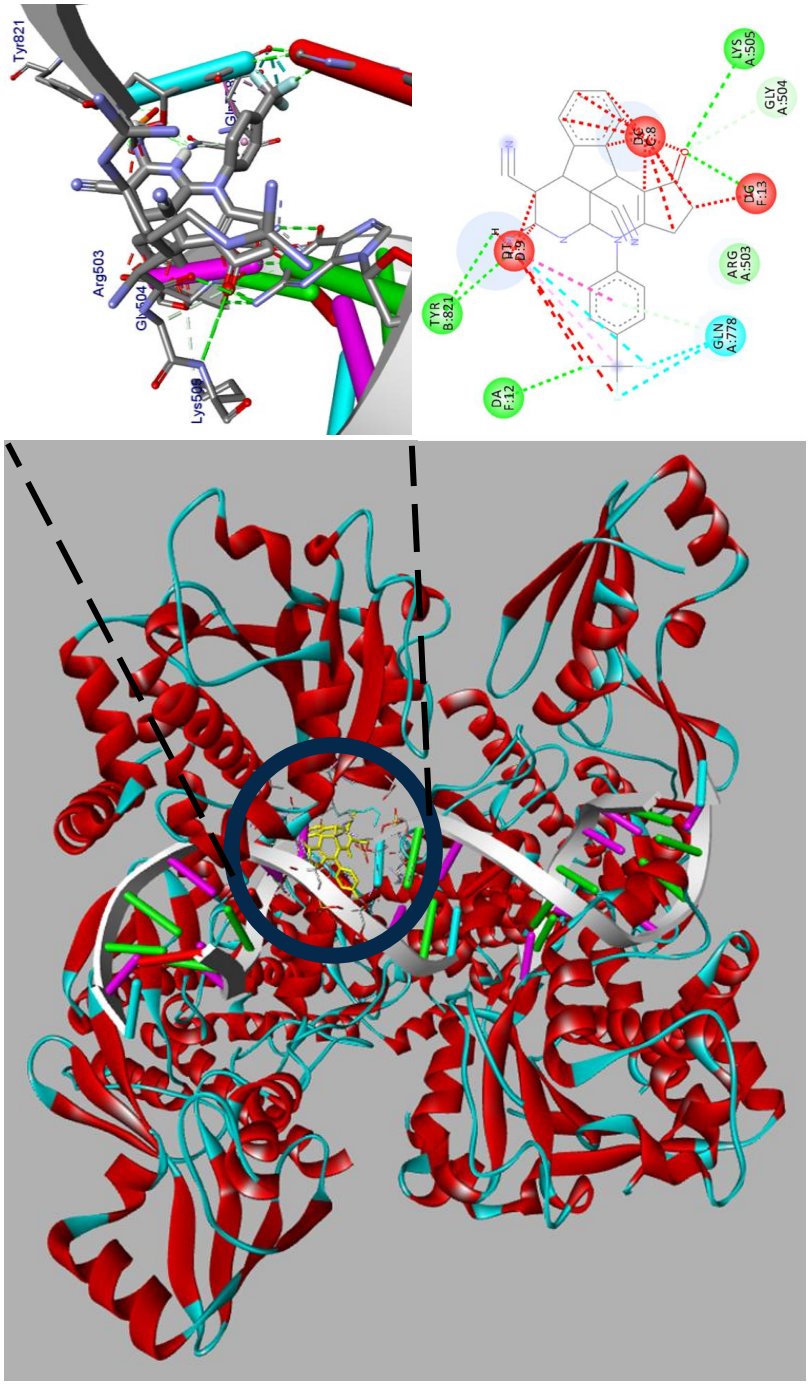

Figure S28: The 2D and 3D binding interactions of compound **6i** against human topoisomerase IIβ (PDB ID: 3QX3). 3D Ribbon model shows the binding pocket structure of human topoisomerase IIβ with compound **6i**. Hydrogen bond between compounds and amino acids are shown as green dash lines, hydrophobic interactions are shown as pink lines.

7. The 2D and 3D binding interactions of Ciprofloxacin and all synthesized compounds (6a-i) against *E.coli* DNA gyraseB (PDB ID: 6F86)

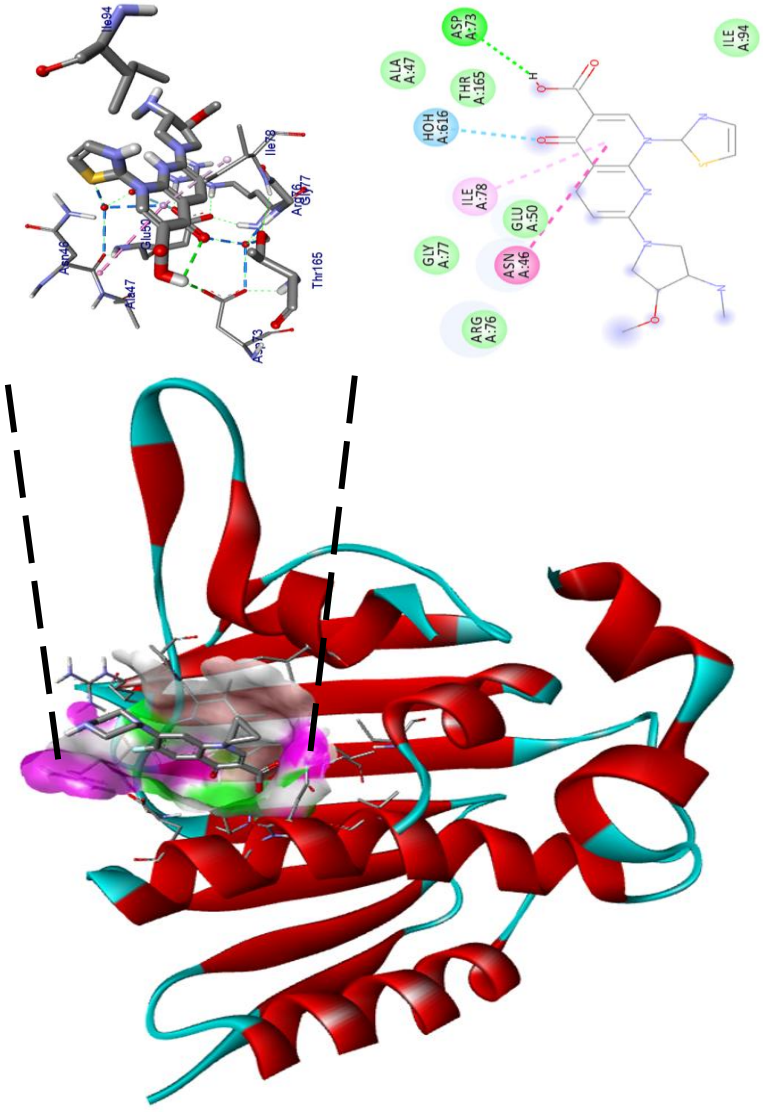

Figure S29: The 2D and 3D binding interactions of **Ciprofloxacin** against *E.coli* DNA gyraseB (PDB ID: 6F86). 3D Ribbon model shows the binding pocket structure of *E.coli* DNA gyraseB with **Ciprofloxacin**. Hydrogen bond between compounds and amino acids are shown as green dash lines, hydrophobic interactions are shown as pink lines.

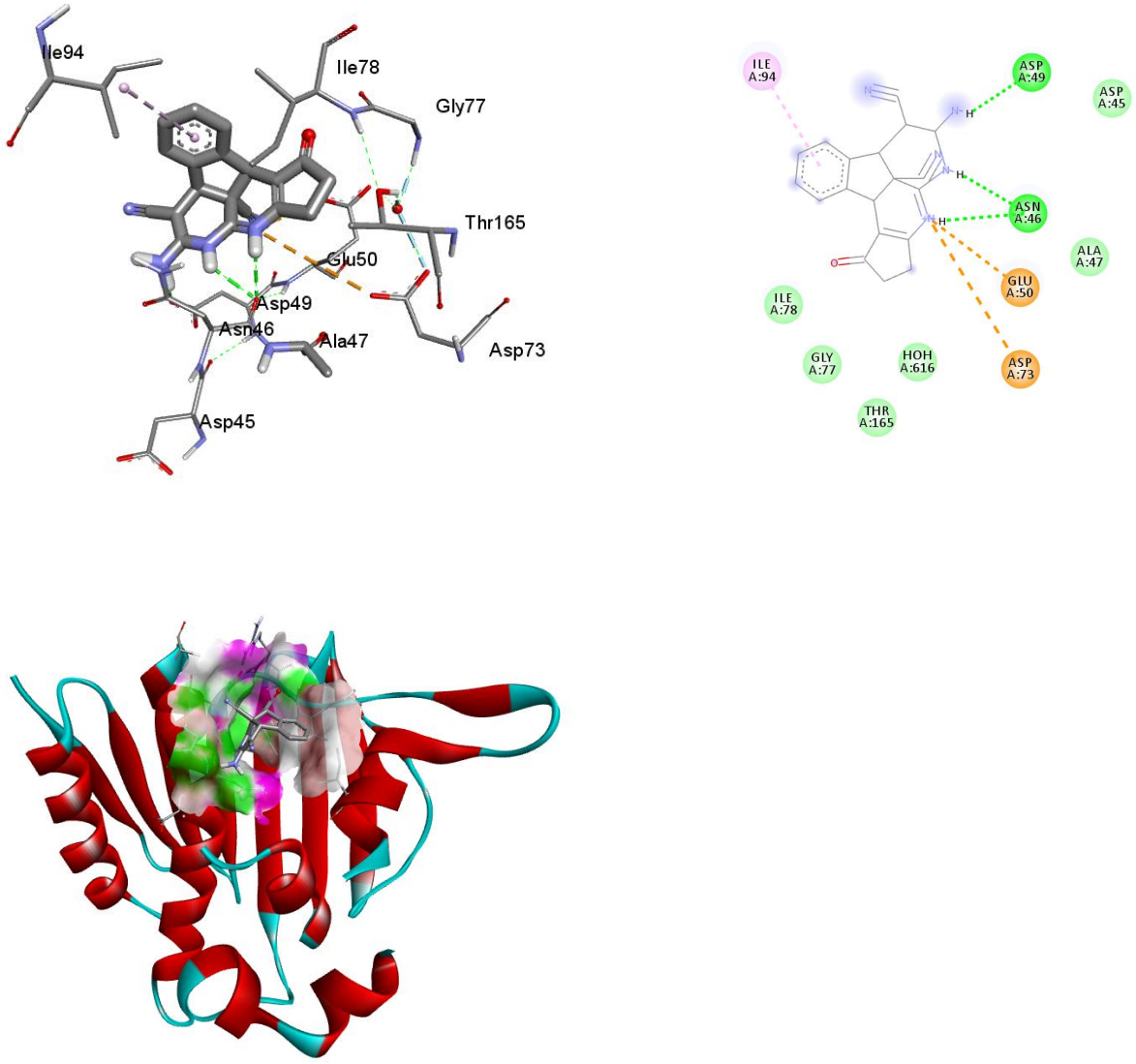

Figure S30: The 2D and 3D binding interactions of compound **6a** against *E.coli* DNA gyraseB (PDB ID: 6F86). 3D Ribbon model shows the binding pocket structure of *E.coli* DNA gyraseB with compound **6a**. Hydrogen bond between compounds and amino acids are shown as green dash lines, hydrophobic interactions are shown as pink lines.

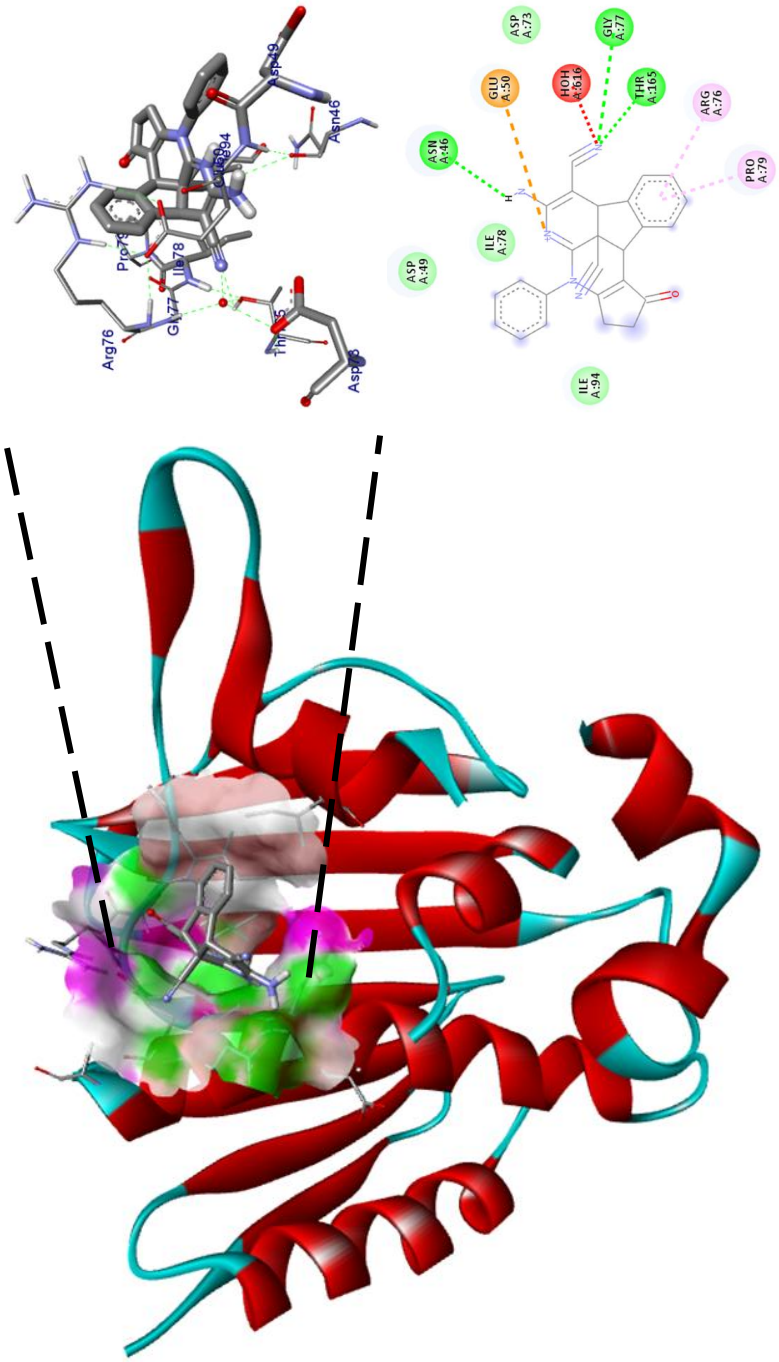

Figure S31: The 2D and 3D binding interactions of compound **6b** against *E.coli* DNA gyraseB (PDB ID: 6F86). 3D Ribbon model shows the binding pocket structure of *E.coli* DNA gyraseB with compound **6b**. Hydrogen bond between compounds and amino acids are shown as green dash lines, hydrophobic interactions are shown as pink lines.

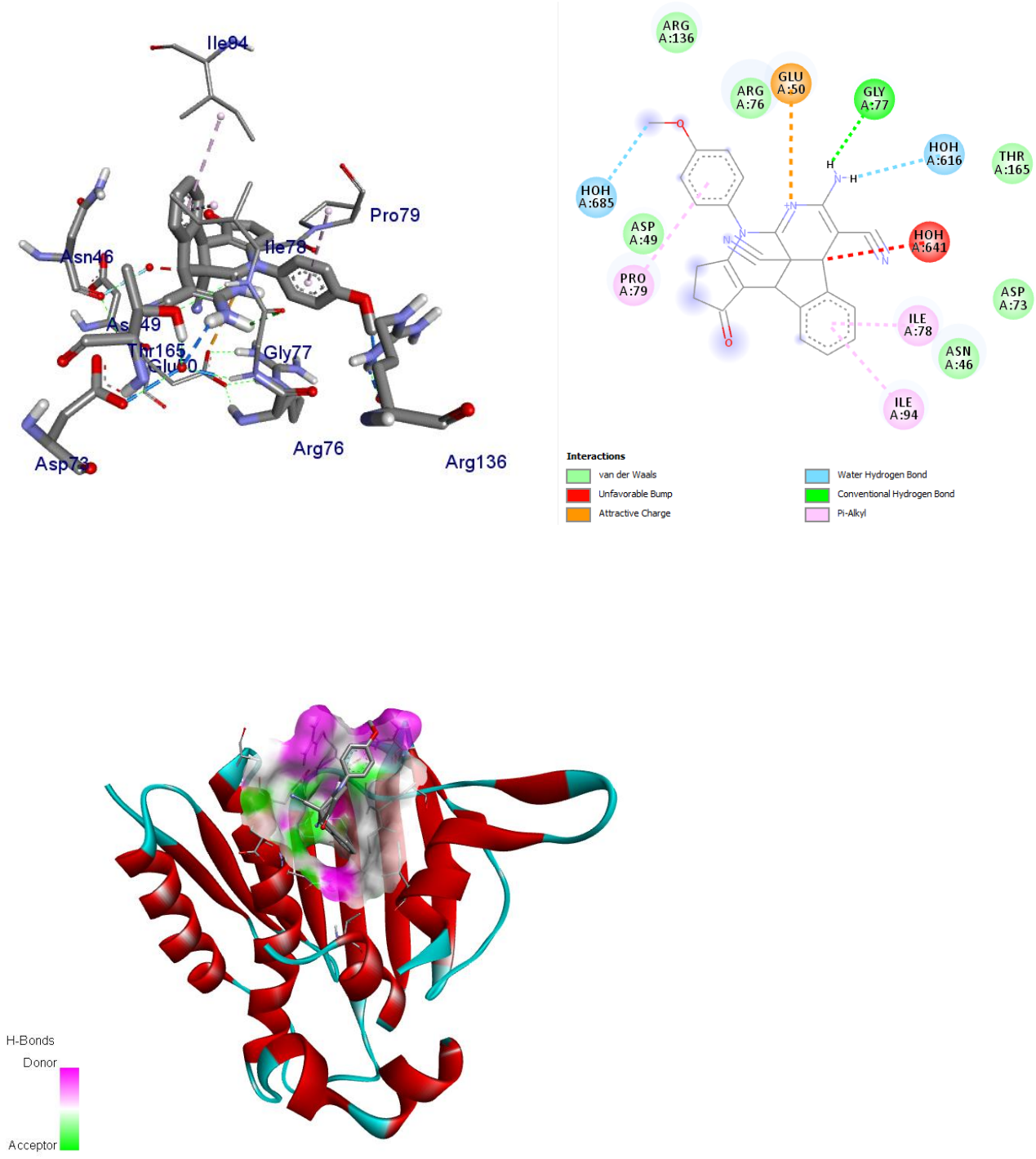

Figure S32: The 2D and 3D binding interactions of compound **6c** against *E.coli* DNA gyraseB (PDB ID: 6F86). 3D Ribbon model shows the binding pocket structure of *E.coli* DNA gyraseB with compound **6c**. Hydrogen bond between compounds and amino acids are shown as green dash lines, hydrophobic interactions are shown as pink lines.

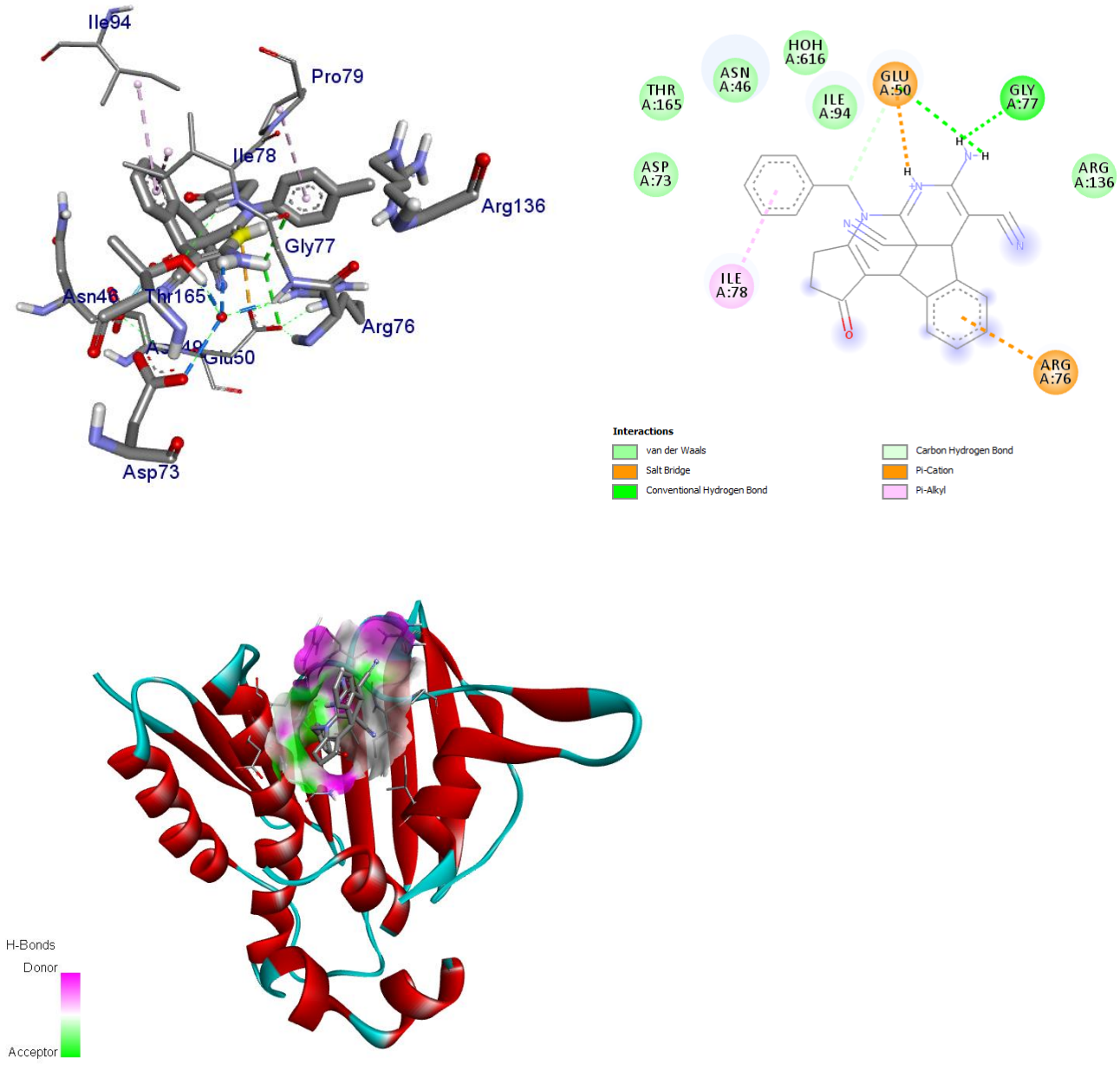

Figure S33: The 2D and 3D binding interactions of compound **6d** against *E.coli* DNA gyraseB (PDB ID: 6F86). 3D Ribbon model shows the binding pocket structure of *E.coli* DNA gyraseB with compound **6d**. Hydrogen bond between compounds and amino acids are shown as green dash lines, hydrophobic interactions are shown as pink lines.

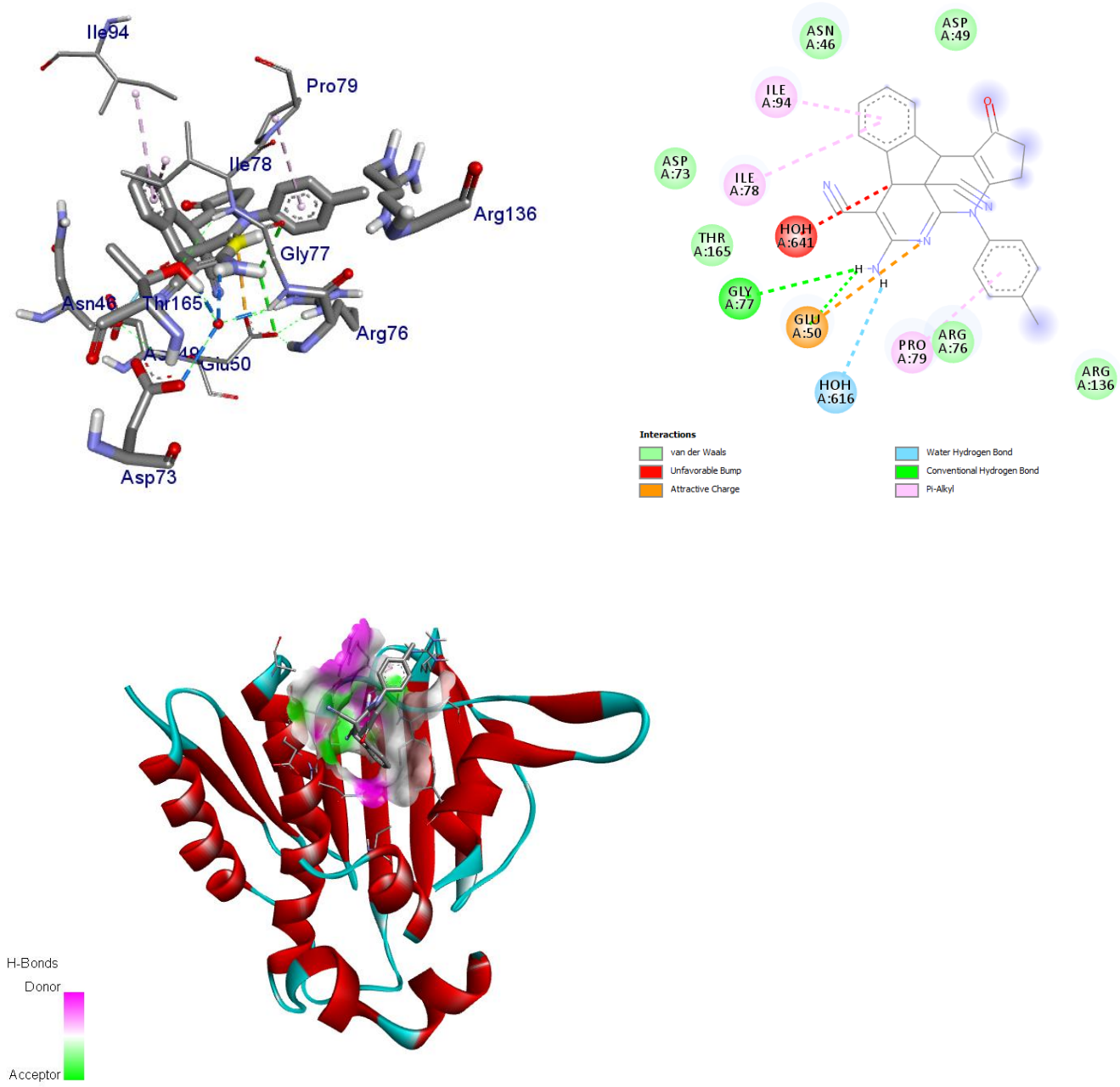

Figure S34: The 2D and 3D binding interactions of compound **6e** against *E.coli* DNA gyraseB (PDB ID: 6F86). 3D Ribbon model shows the binding pocket structure of *E.coli* DNA gyraseB with compound **6e**. Hydrogen bond between compounds and amino acids are shown as green dash lines, hydrophobic interactions are shown as pink lines.

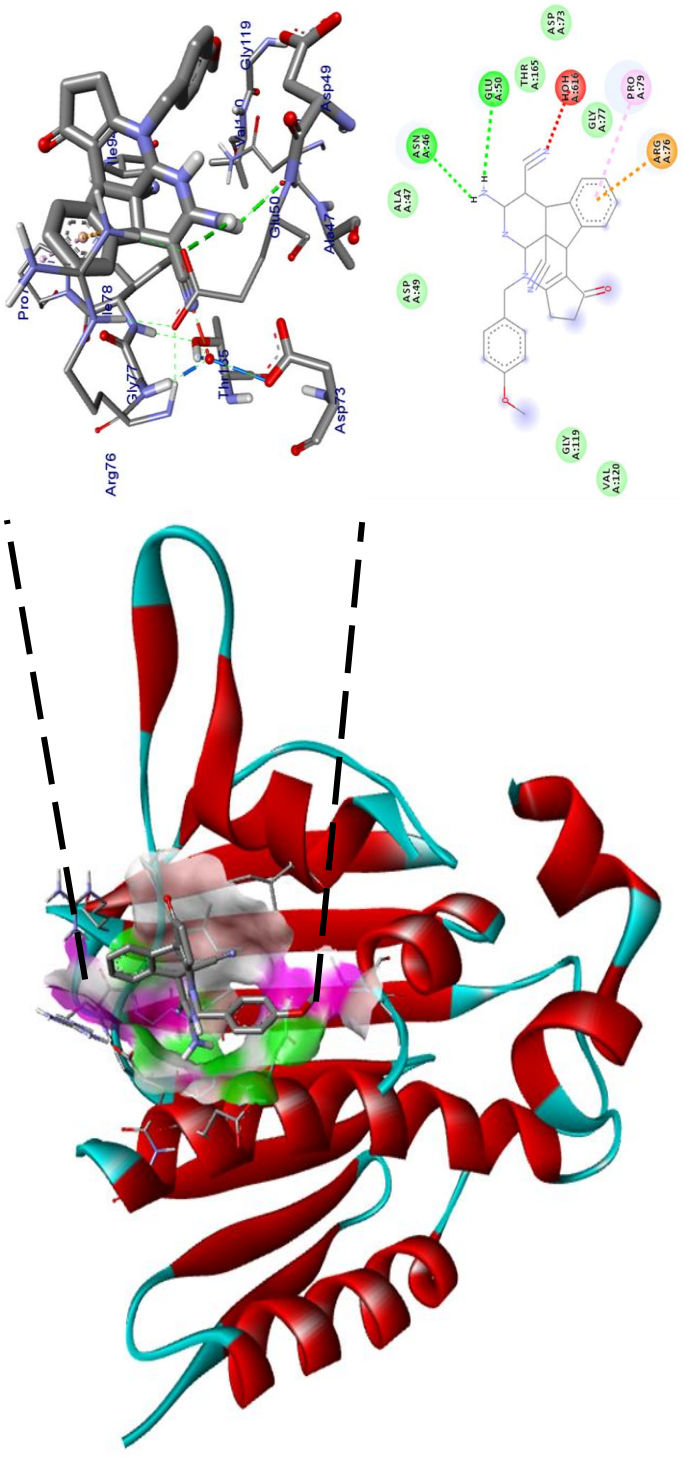

Figure S35: The 2D and 3D binding interactions of compound **6f** against *E.coli* DNA gyraseB (PDB ID: 6F86). 3D Ribbon model shows the binding pocket structure of *E.coli* DNA gyraseB with compound **6f**. Hydrogen bond between compounds and amino acids are shown as green dash lines, hydrophobic interactions are shown as pink lines.

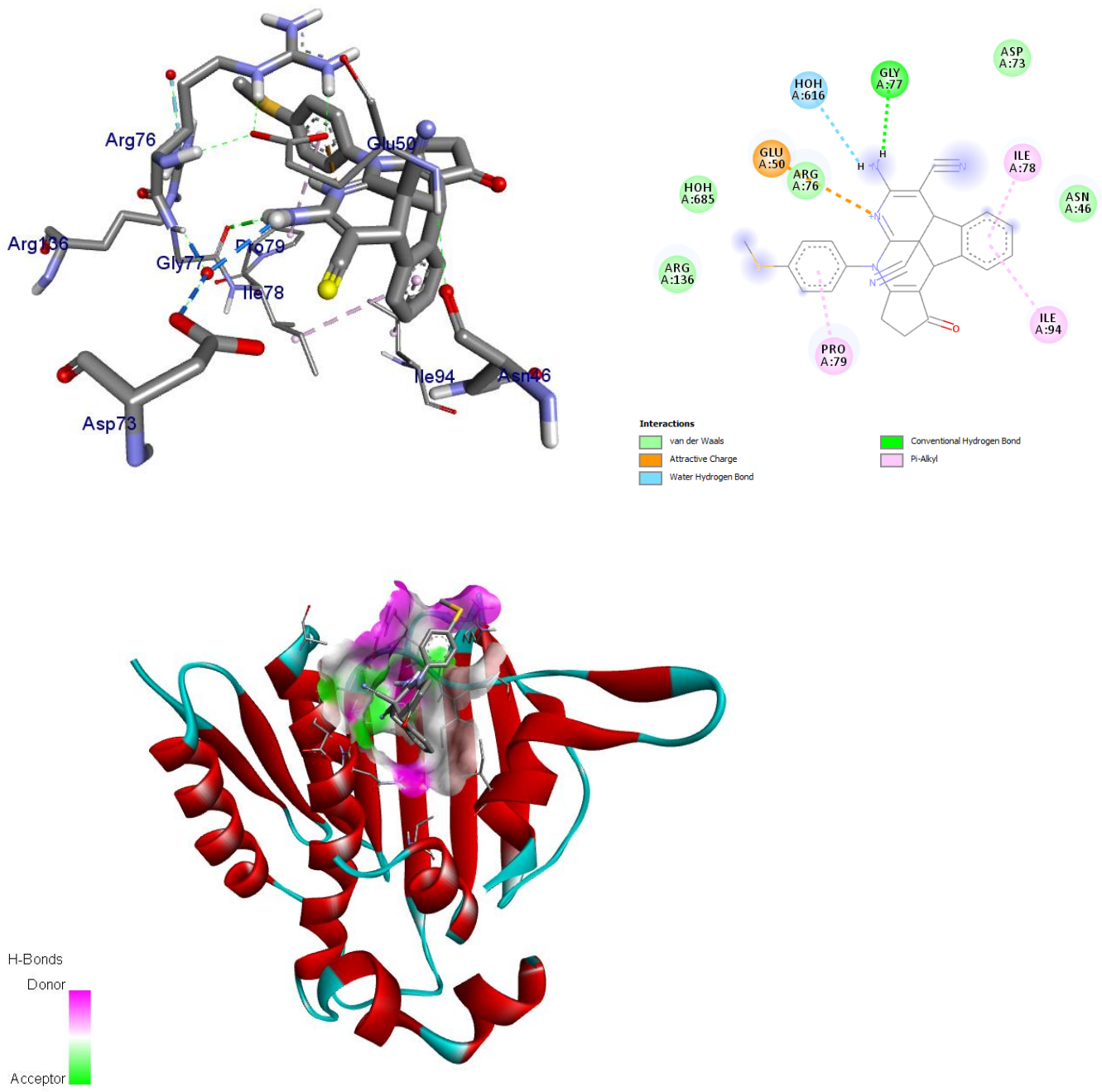

Figure S36: The 2D and 3D binding interactions of compound **6g** against *E.coli* DNA gyraseB (PDB ID: 6F86). 3D Ribbon model shows the binding pocket structure of *E.coli* DNA gyraseB with compound **6g**. Hydrogen bond between compounds and amino acids are shown as green dash lines, hydrophobic interactions are shown as pink lines.

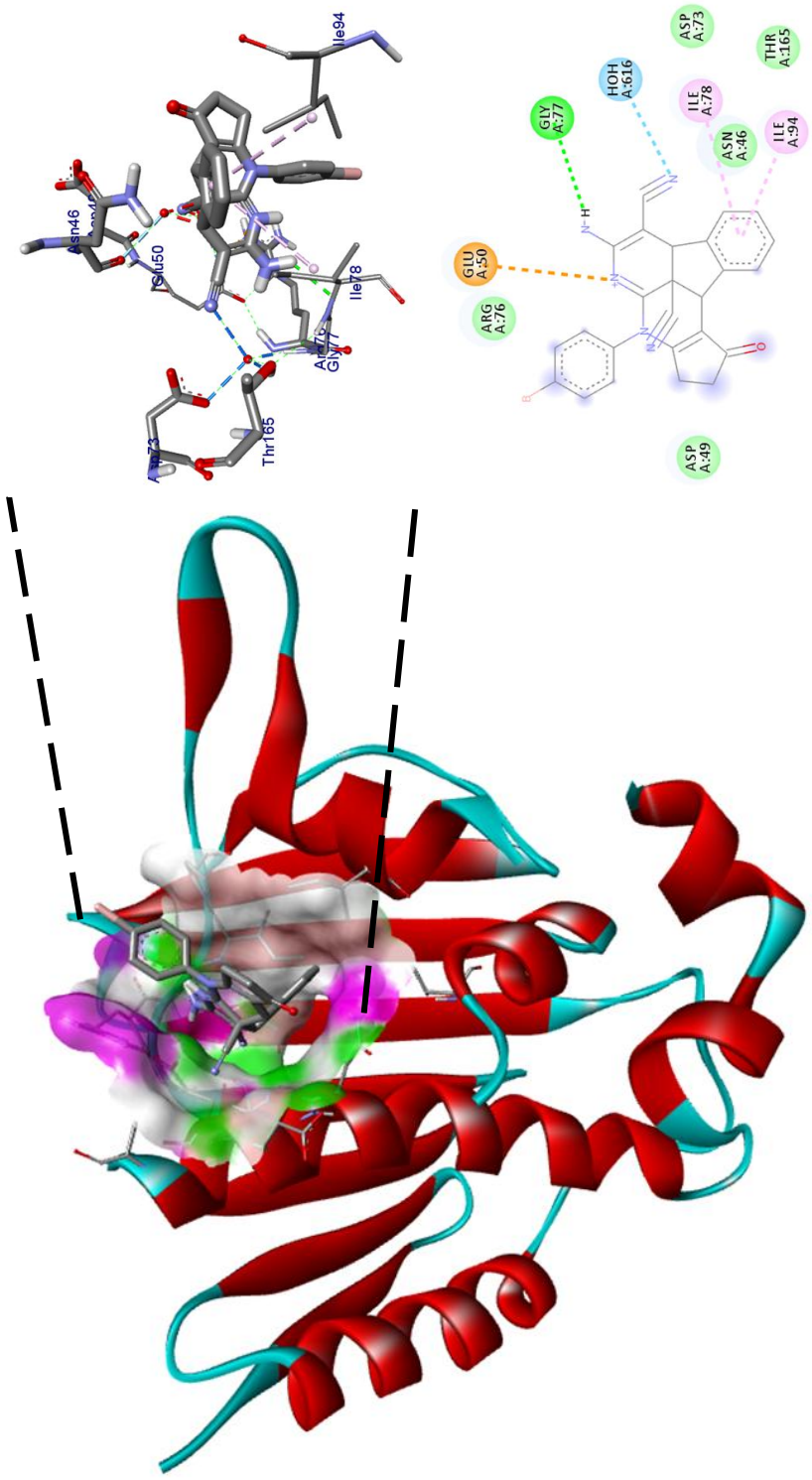

Figure S37: The 2D and 3D binding interactions of compound **6h** against *E.coli* DNA gyraseB (PDB ID: 6F86). 3D Ribbon model shows the binding pocket structure of *E.coli* DNA gyraseB with compound **6h**. Hydrogen bond between compounds and amino acids are shown as green dash lines, hydrophobic interactions are shown as pink lines.

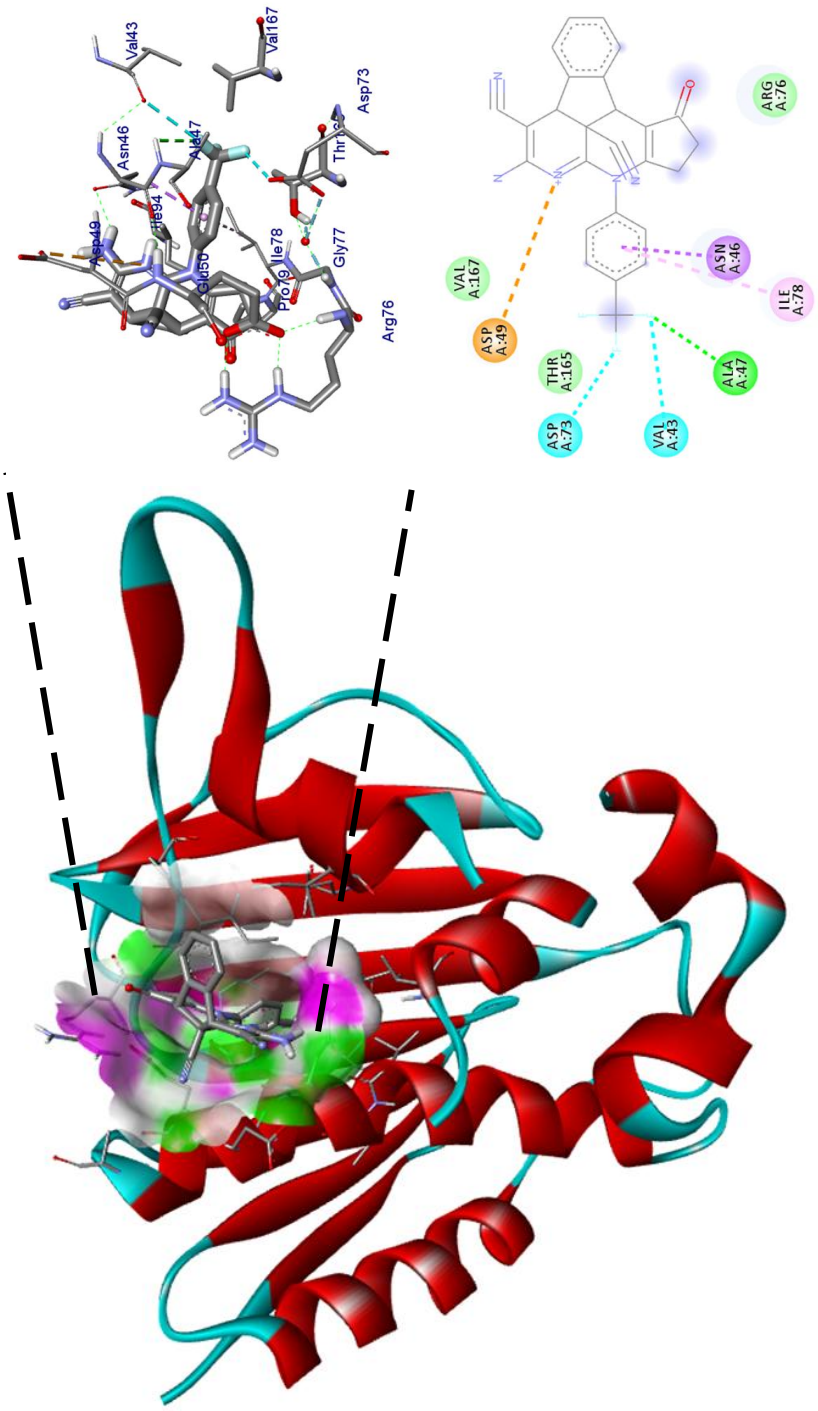

Figure S38: The 2D and 3D binding interactions of compound **6i** against *E.coli* DNA gyraseB (PDB ID: 6F86). 3D Ribbon model shows the binding pocket structure of *E.coli* DNA gyraseB with compound **6i**. Hydrogen bond between compounds and amino acids are shown as green dash lines, hydrophobic interactions are shown as pink lines.